DESIGN OF MICROWAVE NON-REDUNDANT BAND-PASS FILTER USING MICROSTRIP AND EDGE COUPLED SECTIONS

by

VINOJ VIJAYAN PILLAI

Presented to the Faculty of the Graduate School of

The University of Texas at Arlington in Partial Fulfillment

of the Requirements

for the Degree of

MASTER OF SCIENCE IN ELECTRICAL ENGINEERING

THE UNIVERSITY OF TEXAS AT ARLINGTON

December 2009

ACKNOWLEDGEMENTS

I am grateful to Dr. Alan Davis for his patience, guidance, and support throughout my master's program. His passion for research and teaching is truly inspirational, and it is a pleasure working under his leadership. He has invested a lot of time and energy in guiding through my program here at University of Texas at Arlington.

I would also like to thank my committee members, Dr. Jonathan Bredow and Dr. Kambiz Alavi for their continued support and interest in my thesis

I acknowledge the help of Dr.Partha Ghosh and my fellow doctorate student Harvijay Singh for their guidance in this work. I would also like to thank my friends in electrical department especially Vineeth Shetty, Ganesh Krishnamurthy, Rakesh Kalathil, Arun Thomas and Sreejith for their valuable comments and suggestions at various stages of my work.

Finally, I would like to thank my family and friends for their support and encouragement.

November 20, 2009

ABSTRACT

DESIGN OF MICROWAVE NON-REDUNDANT BAND-PASS
FILTER USING MICROSTRIP AND EDGE
COUPLED SECTIONS

Vinoj Pillai, M.S.

The University of Texas at Arlington, 2009

Supervising Professor: Dr. Alan Davis

Microwave filler design using the non-redundant method relies on using the quarter wave Unit Elements (U.E's) to create a complex pole and hence augment the filter skirt response as against the redundant method wherein the U.E's do not contribute towards the filtering action. Filters realized using this method may have series high impedance capacitors, which are not realizable in planar microstrip technology.

This thesis proposes a method to integrate microstrip transmission line and coupled line elements to circumvent the problem of realizing series capacitance. The total number of transmission line elements required to realize the filter is the minimum number required by the multipole filter. The filter realized in this work is based on the work by Horton and Wenzel [7] on realizing optimum quarter-wave TEM filters. Sonnet software is used to simulate and verify the calculations. The fabricated filter was measured using the network analyzer and the results are included.

TABLE OF CONTENTS

LIST OF FIGURES

LIST OF TABLES

CHAPTER 1

TRANSMISSION LINE FUNDAMENTALS

1.1 The Concept of Impedance

The term impedance was first used by Oliver Heaviside In the nineteenth Century to describe the complex ratio V/I in AC circuits consisting of resistors, inductors, and capacitors. It was then applied to transmission lines, in terms of lumped-element equivalent circuits, distributed series impedance, and shunt admittance of the line. The various types of impedances encountered in the microwave engineering are [1]:

$\eta = \sqrt{\mu/\varepsilon}$ is the intrinsic impedance of the medium. This impedance is dependent only on the material properties of the medium, and is equal to the wave impedance for plane waves.

$Z_w = E_t/H_t$ is the wave impedance. This impedance is a characteristic of the particular type of wave. TEM, TM, and TE waves each have different wave impedances (Z_{TEM}, Z_{TM}, Z_{TE}), which may depend on the type of line or guide, the material and the operating frequency.

$Z_0 = \sqrt{L/C}$ is the characteristic impedance. Characteristic impedance is the ratio of voltage to current for a travelling wave on a transmission line. Characteristic impedance of TEM lines is uniquely defined but not for TE and TM waves since they do not have a uniquely defined voltage or current. Hence the characteristic impedance for such a wave may be defined in various ways.

1.2 Voltage-Current Two-Port Parameters

A linear n-port network is completely characterized by n independent excitation variables and n dependent response variables. These variables are the terminal voltage and currents. There are four ways of arranging these independent and dependant variables in a two-port network. They are the impedance parameters (Z-matrix), admittance parameters (Y-matrix), hybrid parameters (H-matrix) and the inverse hybrid parameters (G-matrix) [3]. These four sets of parameters are defined as:

$$\begin{bmatrix} V_1 \\ V_2 \end{bmatrix} = \begin{bmatrix} Z_{11} & Z_{12} \\ Z_{21} & Z_{22} \end{bmatrix} \begin{bmatrix} I_1 \\ I_2 \end{bmatrix} \tag{1.1a}$$

$$\begin{bmatrix} I_1 \\ I_2 \end{bmatrix} = \begin{bmatrix} Y_{11} & Y \\ Y_{21} & Y_{22} \end{bmatrix} \begin{bmatrix} V_1 \\ V_2 \end{bmatrix} \tag{1.1b}$$

$$\begin{bmatrix} V_1 \\ I_2 \end{bmatrix} = \begin{bmatrix} h_{11} & h_{12} \\ h_{21} & h_{22} \end{bmatrix} \begin{bmatrix} I_1 \\ V_2 \end{bmatrix} \tag{1.1c}$$

$$\begin{bmatrix} I_1 \\ V_2 \end{bmatrix} = \begin{bmatrix} g_{11} & g_{12} \\ g_{21} & g_{22} \end{bmatrix} \begin{bmatrix} V_1 \\ I_2 \end{bmatrix} \tag{1.1d}$$

Two series connected networks can be combined by adding the Z parameters of the individual networks. Two shunt connected networks can be combined by adding their individual Y-matrices. Similarly, when two circuits are connected in series-shunt or shunt-series, the composite matrix can be found by adding the individual *h* or *g* parameters respectively.

1.3 *ABCD* Parameters

ABCD parameters are widely used in systems where two-port networks are connected in cascade. The *ABCD* parameters have the property of having port-1 variables being the independent variables and the port-2 variables being the dependent ones [3].

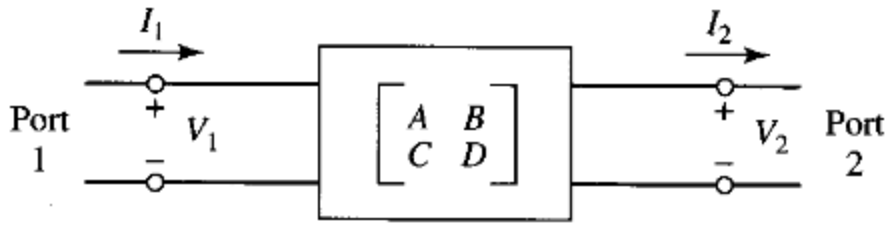

Figure 1.1 Two-port network to be represented by *ABCD* parameters.

The *ABCD* matrix of a simple two-port network can be represented by

$$\begin{bmatrix} V_1 \\ I_1 \end{bmatrix} = \begin{bmatrix} A & B \\ C & D \end{bmatrix} \begin{bmatrix} V_2 \\ -I_2 \end{bmatrix} \tag{1.2}$$

This allows the cascade of two networks to be represented as the matrix product of two circuits expressed in terms of *ABCD* parameters. Consider a pair of two-port networks as shown in Figure 1.2. Network 1 is characterized by parameters A_1, B_1, C_1, D_1 and network 2 is characterized by parameters A_2, B_2, C_2, D_2. Note that I_2 is directed away from network 1. Hence the equations can be written as,

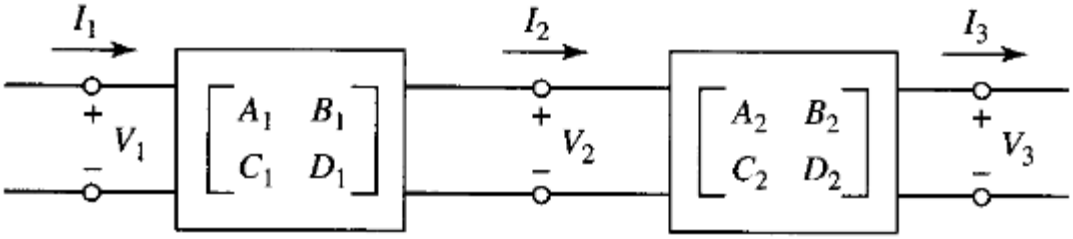

Figure 1.2 Two cascaded two-port networks.

$$\begin{bmatrix} V_1 \\ I_1 \end{bmatrix} = \begin{bmatrix} A_1 & B_1 \\ C_1 & D_1 \end{bmatrix} \begin{bmatrix} V_2 \\ I_2 \end{bmatrix} \tag{1.3a}$$

$$\begin{bmatrix} V_2 \\ I_2 \end{bmatrix} = \begin{bmatrix} A_2 & B_2 \\ C_2 & D_2 \end{bmatrix} \begin{bmatrix} V_3 \\ -I_3 \end{bmatrix} \tag{1.3b}$$

From (1.3a) and (1.3b),

$$\begin{bmatrix} V_1 \\ I_1 \end{bmatrix} = \begin{bmatrix} A_1 & B_1 \\ C_1 & D_1 \end{bmatrix} \begin{bmatrix} A_2 & B_2 \\ C_2 & D_2 \end{bmatrix} \begin{bmatrix} V_3 \\ -I_3 \end{bmatrix} \tag{1.4}$$

which is of the form

$$\begin{bmatrix} V_1 \\ I_1 \end{bmatrix} = \begin{bmatrix} A & B \\ C & D \end{bmatrix} \begin{bmatrix} V_3 \\ -I_3 \end{bmatrix} \tag{1.5}$$

This proves that *ABCD* matrix of the cascade connection of two networks is equal to the product of the *ABCD* matrices representing the individual two-ports. Libraries of these *ABCD* matrices for elementary two-ports can be used in building block fashion to produce more complicated microwave networks. The attached Figure 1.3 tabulates the ABCD parameters of some commonly used two-ports, Pozar [1].

Circuit	*ABCD* Parameters	
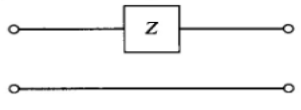	$A = 1$ $C = 0$	$B = Z$ $D = 1$
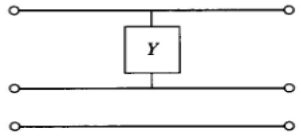	$A = 1$ $C = Y$	$B = 0$ $D = 1$
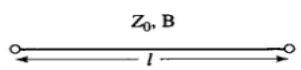	$A = \cos\beta\ell$ $C = jY_0 \sin\beta\ell$	$B = jZ_0 \sin\beta\ell$ $D = \cos\beta\ell$
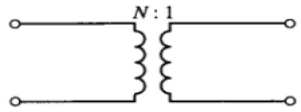	$A = N$ $C = 0$	$B = 0$ $D = \frac{1}{N}$
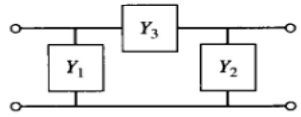	$A = 1 + \frac{Y_2}{Y_3}$ $C = Y_1 + Y_2 + \frac{Y_1 Y_2}{Y_3}$	$B = \frac{1}{Y_3}$ $D = 1 + \frac{Y_1}{Y_3}$
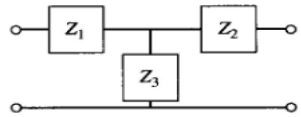	$A = 1 + \frac{Z_1}{Z_3}$ $C = \frac{1}{Z_3}$	$B = Z_1 + Z_2 + \frac{Z_1 Z_2}{Z_3}$ $D = 1 + \frac{Z_2}{Z_3}$

Figure 1.3 ABCD Parameters of some useful two-port circuits. Pozar [1].

1.4 Image Impedance

The optimum generator impedance for a two-port circuit shown in

Figure 1.4 depends on both the two-port and its load impedance. Also, the matched load impedance at the output side will depend on the two-port as well as on the generator impedance on the input side.

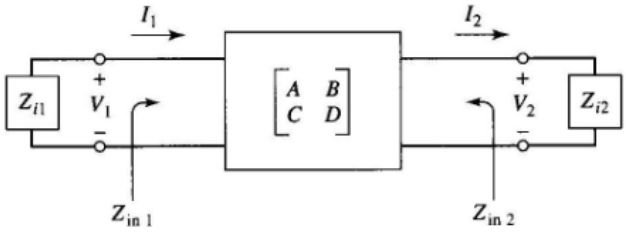

Figure 1.4 Excitation of a two-port at port-1.

-

Both sides are matched simultaneously when the input side is terminated with an impedance equal to its image impedance, Z_{I1} and the output side terminated with a load impedance equal to Z_{I2}. The actual values of Z_{I1} and Z_{I2} are determined completely by the two-port circuit itself and are independent of the loading on either side of the circuit. Terminating the two-port circuit in this way will guarantee maximum power transfer from the generator to the output side and maximum power transfer from a generator at the output side (if it exists) to the input side [3].

The image impedance in terms of *ABCD* parameters can be defined as:

$$Z_{I1} = \sqrt{AB/CD} \tag{1.6a}$$

$$Z_{I2} = \sqrt{DB/AC} \tag{1.6b}$$

The image impedance can also be written in terms of the open circuit Z parameters and short circuit Y parameters.

$$Z_{I1} = \sqrt{z_{11}/y_{11}} = \sqrt{z_{oc1}z_{sc1}} \tag{1.7a}$$

$$Z_{I2} = \sqrt{z_{22}/y_{22}} = \sqrt{z_{oc2}z_{sc2}} \tag{1.7b}$$

where z_{oc1}, z_{sc1} are the input impedances when the output port is an open or short circuit, respectively.

1.5 S-Parameters

The *Z* or *Y* parameters are not used for measurements at high frequencies since they are difficult to measure for the following reasons.

a) It is difficult to measure voltages and currents at high frequencies.

b) It is necessary to use open and short circuits in order to find *Z and Y* parameters, which at microwave frequencies may cause instability when active elements are involved.

S parameters are defined with respect to incident and reflected power, which can be measured easily at high frequencies. S parameters denote the fraction of incident power reflected at a port and transmitted to other ports. The addition of phase information allows the complete description of any linear circuit. Referring to Figure 1.5, the incident voltage wave a_n and the reflected normalized voltage wave b_n are defined as follows.

$$a_n = \frac{1}{2\sqrt{Z_0}}(V_n + Z_0 I_n) \tag{1.8a}$$

$$b_n = \frac{1}{2\sqrt{Z_0}}(V_n - Z_0 I_n) \tag{1.8b}$$

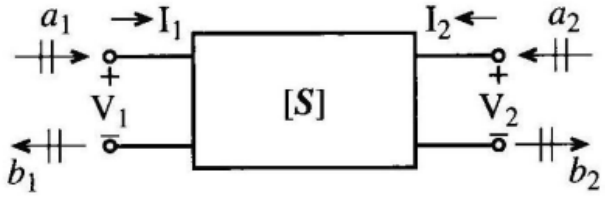

Figure 1.5 Convention for defining *S*-Parameters [5].

Where the index *n* refers to either port 1 or 2. The impedance Z_0 is the characteristic impedance of the connecting lines on the input and output side of the network. The voltage and current at any point along the transmission line can be expressed in terms of forward and reverse travelling waves. Thus,

$$V_n = V_n^+ + V_n^- = \sqrt{Z_{0n}}(a_n + b_n) \tag{1.9}$$

$$I_n = I_n^+ - I_n^- = \frac{(a_n + b_n)}{\sqrt{Z_{0n}}} \tag{1.10}$$

The *S*-Parameters for a two-port network are defined as:

$$\begin{Bmatrix} b_1 \\ b_2 \end{Bmatrix} = \begin{bmatrix} S_{11} & S_{12} \\ S_{21} & S_{22} \end{bmatrix} \begin{Bmatrix} a_1 \\ a_2 \end{Bmatrix} \tag{1.11}$$

where the terms are

$$S_{11} = {b_1}/{a_1}\Big|_{a_2=0} = \frac{\text{reflected voltage wave at port 1}}{\text{incident voltage wave at port 1}} \tag{1.12}$$

$$S_{21} = {b_2}/{a_1}\Big|_{a_2=0} = \frac{\text{transmitted voltage wave at port 2}}{\text{incident voltage wave at port 1}} \tag{1.13}$$

$$S_{22} = {b_2}/{a_2}\Big|_{a_1=0} = \frac{\text{reflected voltage wave at port 2}}{\text{incident voltage wave at port 2}} \tag{1.14}$$

$$S_{12} = {b_1}/{a_2}\Big|_{a_1=0} = \frac{\text{transmitted voltage wave at port 1}}{\text{incident voltage wave at port 2}} \tag{1.15}$$

1.6 Transmission Line Equation

A transmission line is characterized by its mechanical length, *L*, and its characteristic impedance Z_0. The characteristic impedance of a transmission line is a function only of the geometry and dielectric constant of the material between the lines and is independent of its terminating impedances. For a lossless transmission line, the characteristic impedance and the propagation constant can be found to be:

$$Z_0 = \sqrt{L/C} \tag{1.16}$$

$$\beta = \omega\sqrt{LC} \tag{1.17}$$

where L and C are inductance and capacitance per unit length of the transmission line.

The input impedance of a lossless transmission line terminated in a load impedance of Z_L is given by :

$$Z_{in} = Z_0 \frac{Z_L + j Z_0 tan\beta l}{Z_0 + j Z_L tan\beta l} \tag{1.18}$$

1.7 General Characteristics of TEM and Quasi-TEM Modes

Any two conductor lossless transmission lines placed in a homogenous dielectric medium supports a pure TEM mode of propagation. Some common examples of this type of transmissions are twin-wire, coaxial, and shielded stripline. If a two-conductor transmission line is enclosed in an inhomogeneous dielectric medium, the mode of propagation is pure-TEM only in the limit of zero frequency. Examples of such transmission lines are microstrip, slot line and coplanar waveguide (CPW).

The characteristic impedance and complex propagation constant of a TEM or a quasi-TEM mode transmission line can be described in terms of basic parameters of the line (i.e, its per unit length resistance R, inductance L, capacitance C, and conductance G). The equivalent circuit of a transmission line of length $\triangle z$ is shown below.

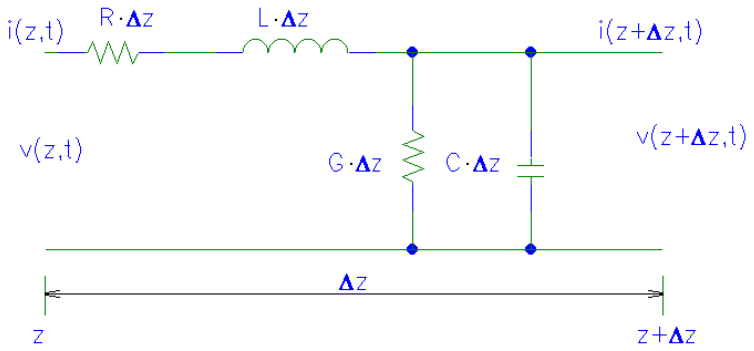

Figure 1.6 Equivalent circuit for an incremental length of transmission line.

In terms of parameters R, G, L, C expressed in unit length, the characteristic impedance and the propagation constant γ of a transmission line are given by

$$Z_0 = \sqrt{\frac{R+j\omega L}{G+j\omega C}} \tag{1.19}$$

$$\gamma = \sqrt{(R+j\omega L)(G+j\omega C)} \tag{1.20}$$

At microwave frequencies, low-loss conditions ωL>> R and ωC>> G are usually satisfied for transmission lines conductors fabricated out of normal metals and enclosed in a low dielectric loss medium. Equations (1.11) and (1.12) reduces to

$$Z_0 = \sqrt{\frac{L}{C}} \tag{1.21}$$

$$\gamma = j\omega\sqrt{LC}\left[1+\frac{R}{2j\omega L}+\frac{G}{2j\omega C}\right] \tag{1.22}$$

By substituting (1.19) in to (1.20), the complex propagation constant γ can also be expressed as [9], [12],

$$\gamma = \alpha + j\beta = \frac{1}{2}\left(\frac{R}{Z_0}+GZ_0\right)+j\omega\sqrt{LC} \tag{1.23}$$

where ω = 2πf denotes the angular frequency. From (1.17):

$$\beta = \frac{\omega}{vp} = \omega\sqrt{LC} \text{ rad/unit length} \tag{1.24}$$

where β and v_p denotes the phase constant and phase velocity, respectively, along the direction of propagation. The attenuation constant is given by

$$\alpha = \frac{1}{2}\left(\frac{R}{Z_0} + GZ_0\right) \text{ Np/unit length} \tag{1.25}$$

It is common to express the attenuation in decibels (dB) rather than in nepers (Np). The loss in dB is obtained by multiplying the loss in Np by 8.686. The attenuation of the transmission line can therefore be also be expressed as

$$\alpha = 4.343\left(\frac{R}{Z0} + GZ_0\right) \text{ dB/unit length} \tag{1.26}$$

Eliminating L from (1.21) and (1.24),

$$Z_0 = \frac{1}{v_p\, C} \tag{1.27}$$

The above equation shows that the characteristic impedance of a transmission line is related to the phase velocity along the transmission line and the capacitance (per unit length) between the conductors of the transmission line. It is also possible to express the phase velocity in terms of the ratio of the actual capacitance of the transmission line to the capacitance of the same transmission line obtained by assuming the dielectric constant of the medium in which it is placed to be unity. Therefore the problem of determining the characteristic impedance and phase velocity of the structure reduces essentially to the problem of finding the capacitance of the structure.

1.8 Reflection Coefficient

The reflection coefficient describes the amplitude of a reflected wave relative to an incident wave. When a transmission line is terminated with a non-matching impedance, a standing wave is set up in the transmission line where the forward- and backward-going voltages and currents are indicated in Figure 1.7 [3].

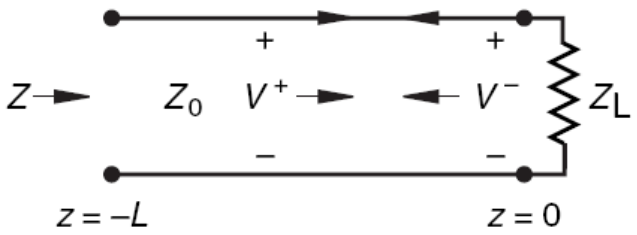

Figure 1.7 Voltage reflections on a terminated transmission line [3].

At the load,

$$V_L = V^+ + V^- \tag{1.28}$$

$$I_L = I^+ - I^- \tag{1.29}$$

Since the forward current wave is $I^+ = V^+/Z_0$ and the reverse current wave is $I^- = V^-/Z_0$, the current at the load is

$$I_L = \frac{V^+ - V^-}{Z_0} = \frac{V_L}{Z_L} \tag{1.30}$$

Replacing V_L in equation (1.30) with (1.28), the voltage reflection coefficient can be determined.

$$\Gamma = \frac{V^-}{V^+} = \frac{Z_L - Z_0}{Z_L + Z_0} \tag{1.31}$$

The magnitude of reflection coefficient varies from 0 (no reflection) to 1 (complete reflection). The reflection coefficient is a vector with magnitude and angle. So, a short circuit on a transmission line would have a reflection coefficient of 1 with a phase angle of 180^0. Similarly, an open circuit would have a reflection coefficient of 1 with phase angle of 0^0.

1.9 VSWR

VSWR stands for Voltage Standing Wave Ratio. When a transmission line is terminated in an impedance different than the characteristic impedance of the line, reflections are set up. These reflections cause local voltage maxima and minima along the length of the transmission line. VSWR is defined as

$$VSWR = {V_{max}}/{V_{min}} = {1 + |\Gamma|}/{1 - |\Gamma|} \quad (1.32)$$

VSWR is a real number such that $1 \leq VSWR \leq \infty$, where a VSWR of 1 implies a matched load.

1.10 Return loss

When the load is mismatched with the transmission line feeding it, not all of the available power from the generator is delivered to the load. This "loss" is called return loss (RL) and is defined in dB as

$$RL = -20\ log|\Gamma|\ dB = -20\ log\left[\frac{VSWR-1}{VSWR+1}\right]\ dB \quad (1.33)$$

It can be observed from the above equation that a matched load ($|\Gamma| = 0$) has a return loss of -∞ dB (no reflected power), whereas a total reflection ($|\Gamma| = 1$ has a return loss of 0 dB (all incident power is reflected.

1.11 Propagation constant

The propagation constant of an electromagnetic wave is the measure of the change undergone by the amplitude of the wave as it propagates in a given direction. The quantity being measured can be the voltage or current in a circuit or a field vector such as electric field strength or flux density. The propagation constant γ is given by:

$$\gamma = \alpha + j\beta \quad (1.34)$$

The real part, α is called the attenuation constant, and β is called the phase constant. The attenuation constant α, is measured in nepers per meter (Np). A neper is approximately 8.7 dB. The phase constant β is measured in radians per meter and is defined as

$$\beta = {2\pi}/{\lambda} \quad (1.35)$$

where λ is the wave length.

1.12 Phase velocity and Group velocity

The phase velocity of a wave is the rate at which the phase of the wave propagates in space. This is the speed at which the phase of any one frequency component of the wave travels. The phase velocity v_p of the TEM wave in a nonmagnetic medium ($\mu_r = 1$) can be found via

$$v_p = \frac{\omega}{\beta} = \frac{1}{\sqrt{\mu\varepsilon}} = \frac{1}{\sqrt{\mu_0\varepsilon_0}}\frac{1}{\sqrt{\varepsilon_r}} = \frac{c}{\sqrt{\varepsilon_r}} \tag{1.36}$$

where c is the speed of light, μ_0 is the permeability of free space, $\omega = 2\pi f$, and β is the phase constant. Thus, the phase velocity is reduced as the permittivity of the material goes up.

Group velocity is a measure of the velocity of energy flow and is given by

$$v_g = \frac{d\omega}{d\beta} \tag{1.37}$$

1.13 Group delay

The group delay is the time it takes for information to traverse the network. It is defined as the negative of the rate of change of change of phase with frequency.

$$t_g = -{}^{d\emptyset(\omega)}/_{d\omega} \tag{1.38}$$

It is often desirable to design a filter with nearly linear phase (i.e. $\emptyset = -A\omega$, with A being an arbitrary constant factor). The group delay is then simply a constant $t_g = A$.

1.14 Special cases of lossless terminated lines.

Short-Circuited transmission line

Consider a transmission line section as shown in Figure 1.8, where a line is terminated in a short circuit, $Z_L = 0$.

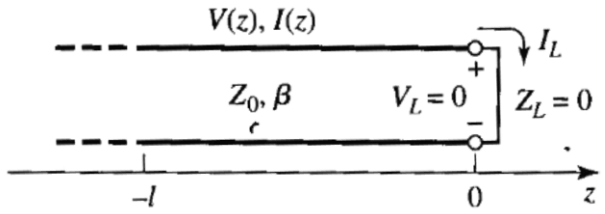

Figure 1.8 A transmission line terminated in a short circuit [1].

From (1.14), the reflection coefficient is $\Gamma = -1$ and from (1.15) the VSWR can be found to be infinite. Substituting $Z_L = 0$ in the equation for input impedance of a lossless transmission line (1.18), gives

$$Z_{in} = jZ_0 \tan \beta l \tag{1.39}$$

The value of Z_{in} can be found to be imaginary for any length l, and it takes values between $+j\infty \; and \; -j\infty$. Equation (1.39) also indicates that the input impedance is periodic in l, repeating for multiples of $\lambda/2$. The voltage, current, and input impedance for the short-circuited line are plotted in Figure 1.9 [1].

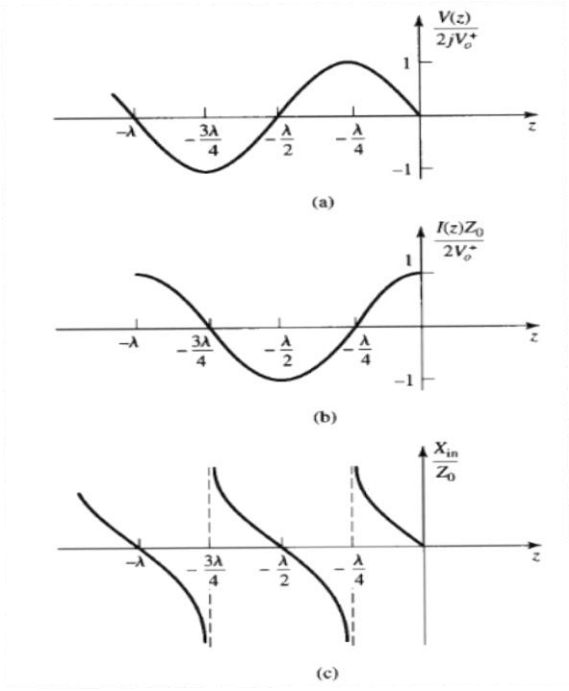

Figure 1.9 a) Voltage, b) current, and c) impedance variation along a short circuited transmission line [1].

Open circuited transmission line.

Consider an open circuited transmission line as shown in Figure 1.10, where $Z_L = \infty$.

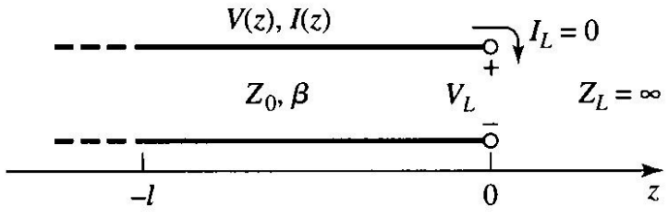

Figure 1.10 A transmission line terminated in an open circuit [1].

The reflection coefficient in this case is found to be $\Gamma = 1$ from (1.31) and the VSWR to be infinite from (1.32). The input impedance for this configuration can be found by substituting $Z_L = \infty$ in (1.18).

Z_{in} can be found to be equal to

$$Z_{in} = -jZ_0 \cot \beta l,$$

which is also purely imaginary for any length l. The voltage, current, and input reactance of the open-circuited are plotted in Figure 1.11.

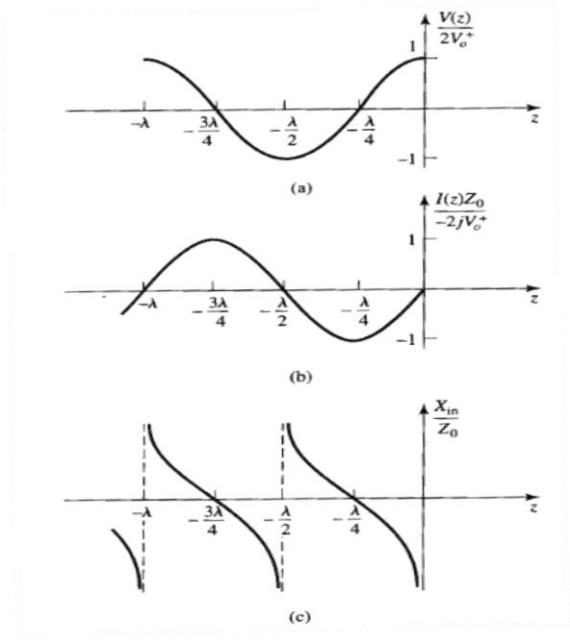

Figure 1.11 a) Voltage, b) current, and c) impedance variation along a short circuited transmission line [1].

Transmission line of length λ/2.

Consider a transmission line of length $l = \lambda/2$ terminated in a load impedance of Z_L . From the expression for the input impedance of a terminated transmission line (1.18), the input impedance can be found to be $Z_{in} = Z_L$. i.e. a half-wavelength line (or any multiple of λ/2) does not alter or transform the load impedance regardless of the characteristic impedance.

Transmission line of length λ/4.

A λ/4 (quarter wave) long line or, more generally, $l = \frac{\lambda}{4} + (2n+1)\lambda/2$, for n=1, 2, 3…equation (1.18) shows that input impedance is given by

$$Z_{in} = {Z_0^2}/{Z_L} \tag{1.40}$$

Such a line is known as quarter-wave transformer because it has the effect of transforming the load impedance, in an inverse manner.

$$Z_0 = \sqrt{Z_{in}\, Z_L} \tag{1.41}$$

Consider Figure 1.12. In order for $\Gamma = 0$, Z_{in} should be equal to Z_0.

Thus, $Z_1 = \sqrt{Z_0 R_L}$

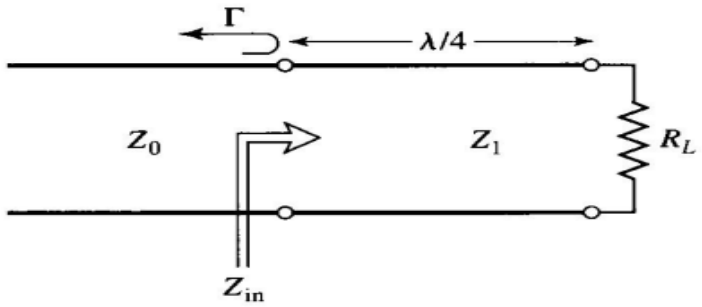

Figure 1.12 The quarter-wave matching transformer [1].

As an example, consider matching an antenna of 75 Ω impedance to an amplifier of 50 Ω impedance using a quarter wave section transmission lines at 8 GHz. Using (1.41) above, the calculated value of the characteristic impedance required to match this turns out to be 61.24Ω. This translates into a line width of approximately 60 mil and length of 280 mil for a Rogers 5880LZ board with a dielectric constant of 1.96. The system is simulated in ADS and the responses are given in Figure 1.14.

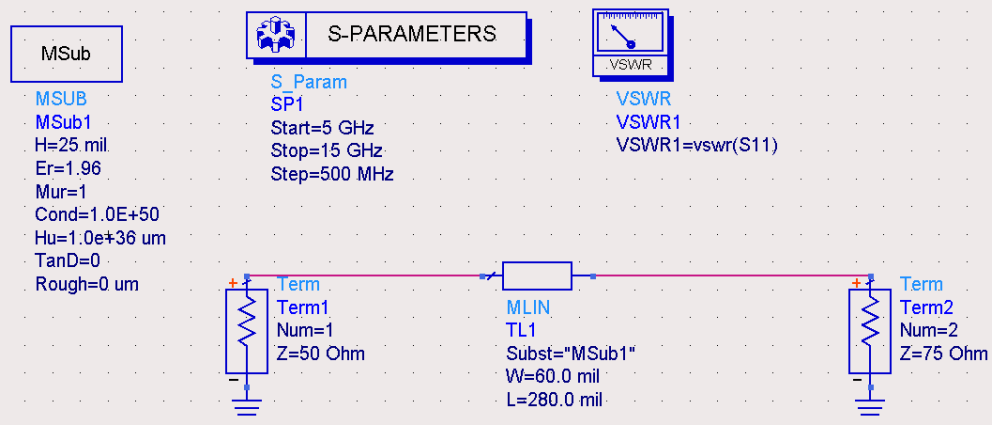

Figure 1.13 Quarter wave transformer simulation.

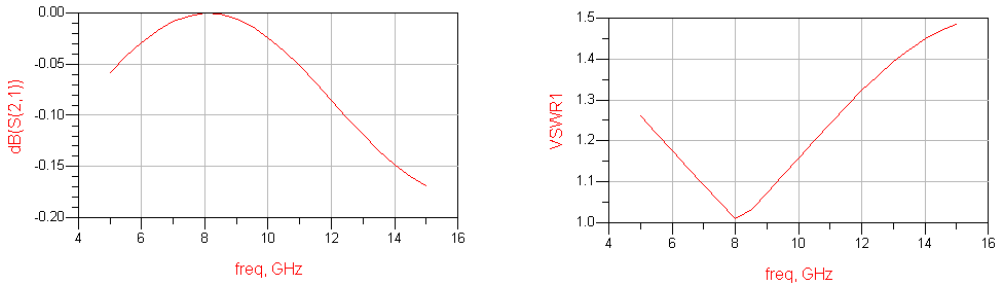

Figure 1.14 S_{21} and VSWR of the matched section.

CHAPTER 2

MICROSTRIP TRANSMISSION LINE

2.1 Microstrip

One of the main requirements for a transmission structure to be suitable as a circuit element in microwave integrated circuits (MICs) is that the structure should be planar in configuration. A planar configuration implies that characteristics of the element can be determined by dimensions in a single plane. There are several transmission structures that satisfy the requirement of being planar. The most common of these are: i) microstrip, ii) coplanar waveguide, iii) slotline, and iv) coplanar strips. A microstrip is the most popular of these transmission structures. The mode of propagation in a microstrip is almost transverse electromagnetic (TEM). This allows easy approximate analysis and yields wide band circuits. The microstrip line has a single upper conductor above an infinite ground plate with a dielectric substrate as carrier. Since microstrip is an open structure, devices can be easily attached to it and post fabrication adjustments can be performed.

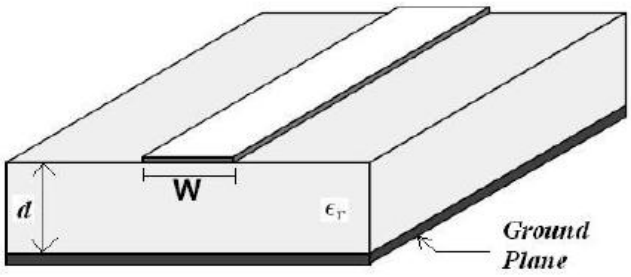

Figure 2.1 Microstrip geometry

There are several variations of the transmission line configuration that are also found in MICs. These include coplanar-waveguide (CPW), inverted microstrip, trapped inverted microstrip and suspended strip line.

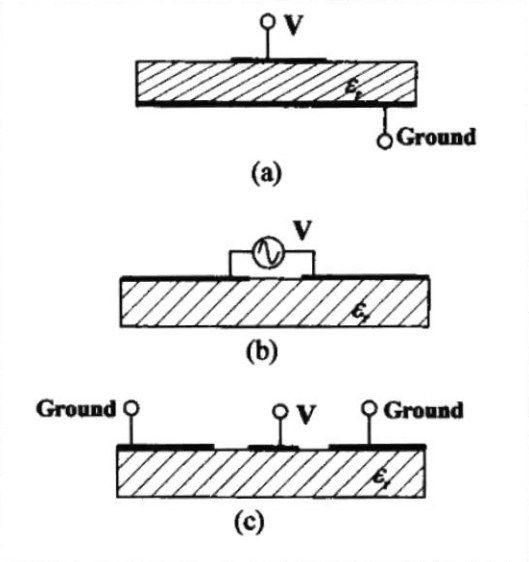

Figure 2.2 Common quasi-TEM mode transmission lines: a) microstrip b) slot line c) coplanar waveguide [9].

The characteristic impedance range of a microstrip is typically 20 Ω to 120 Ω. The upper limit is set by technological constraints on the minimum line width that can be realized and the production tolerances, while the lower limit is essentially set by the appearance of higher order modes. The fabrication of microstrip circuits is relatively simple and done with low-cost technology. The dimensions of microstrip on standard substrates are relatively large, so that the demand for highly precise photolithography is not stringent. Some of the particularly useful characteristics of microstrip include the following [2].

- DC as well as AC signals may be transmitted.
- Active devices, diodes and transistors may be readily incorporated.
- Shunt connections can be made quite easily.
- In-circuit characterization of devices is relatively straight forward to implement.

- Line wave length is reduced considerably (typically one-third) from its free space value, because of the substrate dielectric constant.
- The structure is quite rugged and can with stand moderately high voltage and power levels.

2.1.1 Electromagnetic properties

The microstrip transmission line is an open wave guide structure and its electromagnetic field is theoretically defined in an infinite space. The microstrip is a two-electrode guiding system, and therefore the dominant mode has a zero cutoff frequency. Due to the mixed air-dielectric material, however, the microstrip line cannot propagate a pure transverse electromagnetic (TEM) wave. This is only possible in the special case of air-filled microstrip line. This case is not relevant from a practical point of view, because the strip needs to be suspended in some way.

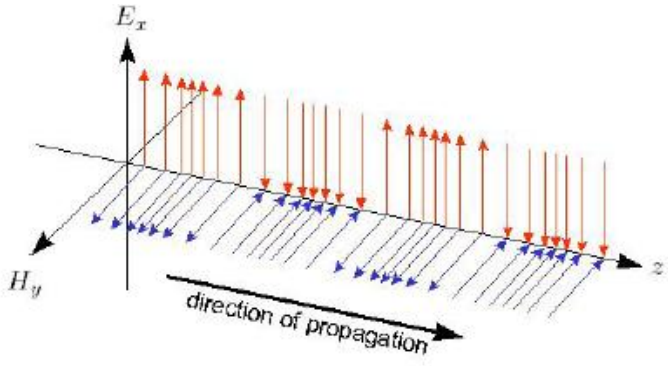

Figure 2.3 An example of TEM propagation [11].

Transmission lines which do not have such a uniform dielectric filling cannot support a pure TEM mode of propagation. Although the bulk of energy which is transmitted along microstrip is with field distribution that closely matches TEM, it is usually referred to as 'quasi-TEM'. Detailed field distribution is quite complicated, but the main transverse electric field can be visualized as shown in Figure 2.4 below [2].

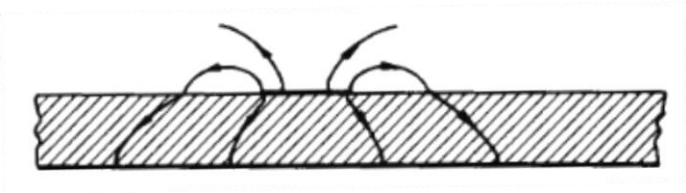

Figure 2.4 Transverse cross section of microstrip showing electric field [2].

2.2 Microstrip synthesis

The microstrip synthesis problem consists of finding the values of width *w* and length *l* corresponding to the characteristic impedance Z_0 and electrical length θ defined at the network design stage. The synthesis yields the normalized width-to-height ratio w/h, as well as a quantity called the effective microstrip permittivity $\varepsilon_{eff.}$ This quantity is unique to mixed-dielectric transmission lines systems and it provides a useful link between mechanical length, impedances, and propagation velocities [2].

For any TEM-type transmission line the characteristic impedance at high frequencies may be expressed in any one of three alternate forms.

$$Z_0 = \sqrt{\frac{L}{C}} \tag{2.1}$$

where, L and C are the inductance and capacitance of the line per unit length of the transmission line.

or

$$Z_0 = v_p\, L \tag{2.2}$$

or

$$Z_0 = \frac{1}{v_p\, C} \tag{2.3}$$

where v_p is the phase velocity of the wave travelling along the line. It is given by

$$v_p = \frac{1}{\sqrt{LC}} \tag{2.4}$$

For an air spaced microstrip line the propagation velocity is given by

$$c = \frac{1}{\sqrt{LC_1}} \tag{2.5}$$

C_1 is the capacitance per unit length for the air filled line. By dividing (1.5) by (1.4), and squaring we obtain

$$\frac{C}{C_1} = \left(\frac{c}{v_p}\right)^2 \tag{2.6}$$

The capacitance ratio, C/C_1, is termed the effective microstrip permittivity ε_{eff}, an important microstrip parameter [2]. A useful relation between Z_0, Z_{01} (characteristic impedance of an air filled microstrip) and ε_{eff} can be derived as

$$Z_0 = \frac{Z_{01}}{\sqrt{\varepsilon_{\text{eff}}}} \text{ or } Z_{01} = Z_0\sqrt{\varepsilon_{\text{eff}}} \tag{2.7}$$

The upper and lower bounds of ε_{eff} can be found by considering the effects of very wide and very narrow lines as indicated in Figure 2.5 below.

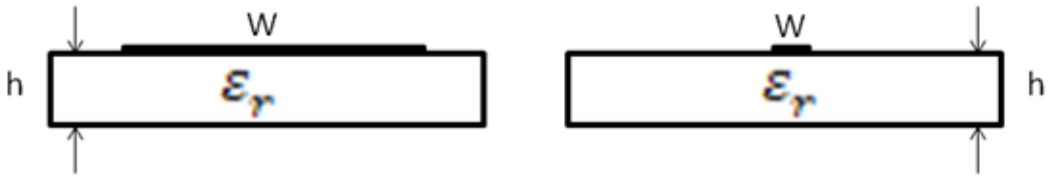

Figure 2.5 Extremely wide (w>>h) and extremely narrow (w<<h) microstrip lines.

For very wide lines, nearly all of the electric field is confined to the substrate dielectric, the structure resembles a parallel plate capacitor, and therefore, at this extreme,

$$\varepsilon_{eff} \rightarrow\rightarrow\rightarrow \varepsilon_r$$

In the case of very narrow lines, the field is almost equally shared by the air ($\varepsilon_r = 1$) and the substrate so that at this extreme,

$$\varepsilon_{eff} \approx {}^1\!/_2\,(\varepsilon_r + 1) \tag{2.8}$$

The range of ε_{eff} is therefore

$$^1/_2\,(\varepsilon_r + 1) \leq \varepsilon_{eff} \leq \varepsilon_r \tag{2.9}$$

2.2.1 Effective dielectric permittivity

The effective dielectric constant can be interpreted as the dielectric constant of a homogenous medium that replaces the air and dielectric regions of the microstrip (Figure 2.6). This accounts for the fact that the fields around the microstrip line are partly in air (lossless) and partly in dielectric [1].

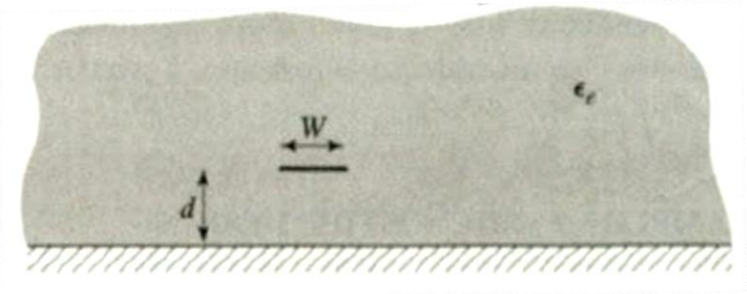

Figure 2.6 Equivalent geometry of quasi-TEM microstrip line [1].

The effective dielectric constant of a microstrip line is approximately given by Pozar [1].

$$\varepsilon_{eff} = \frac{\varepsilon_r+1}{2} + \frac{\varepsilon_r-1}{2}\,\frac{1}{\sqrt{1+12d/W}} \tag{2.10}$$

A few other formulas are given by T Edwards [2] and by Hammerstad and Jenson [16] which are reproduced here as follows

$$\varepsilon_{eff} = \frac{(\varepsilon_r+1)}{2} + \frac{(\varepsilon_r-1)}{2}(1+10/v)^{-ab}, \tag{2.11}$$

where $v = W/d$ and

$$a = 1 + \frac{1}{49}\,ln\left(\frac{v^4+(v/52)^2}{v^4+0.432}\right) + \frac{1}{18.7}\,ln\left(1+\left(\frac{v}{18.1}\right)^3\right), \tag{2.12}$$

$$b = 0.564\left(\frac{\varepsilon_r-0.9}{\varepsilon_r+3}\right)^{0.053} \tag{2.13}$$

The formulas given by Edwards [2], Hammerstad [16] were simulated using MathCAD and compared to simulation done by the program Sonnet. This is shown in Figure 2.7.

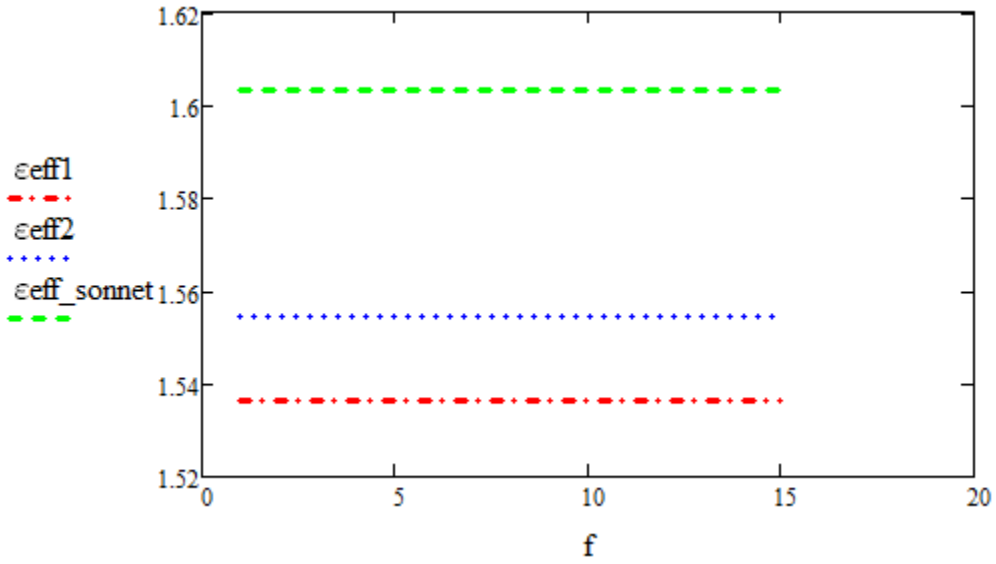

Figure 2.7 Effective dielectric constant $\boldsymbol{\varepsilon_{eff1}}$ is for 1.10 and $\boldsymbol{\varepsilon_{eff2}}$ is for 1.11

For the Sonnet simulation, a 50 Ω line was chosen and $\varepsilon_r = 1.96$ was selected for all the simulations. The Sonnet results are at 1 GHz and the other results are static-TEM approximations.

2.2.2 Microstrip characteristic impedance

Given the dimensions of the microstrip line, characteristic impedance obtained by single-strip static-TEM methods is given by Pozar [1] for two different cases as follows

If $W/d \leq 1$,

$$Z_0 = \frac{60}{\sqrt{\varepsilon_{eff}}} ln\left(\frac{8d}{W} + \frac{W}{4d}\right); \tag{2.14}$$

If $W/d \geq 1$,

$$Z_0 = \frac{120\pi}{\sqrt{\varepsilon_{eff}}[W/d + 1.393 + 0.667\ ln(W/d + 1.444)]}. \tag{2.15}$$

The effect of thickness of conductor is not considered.

2.3 Wavelength λ_g and physical length l

For any propagating wave the velocity is given by the appropriate frequency-wavelength product. In free space we have $c=f\lambda_0$ and in microstrip the velocity is $v_p= f\lambda_g$. The guide wavelength in a mixed dielectric environment is given by

$$\lambda_g = \frac{\lambda_0}{\sqrt{\varepsilon_{eff}}} \tag{2.16}$$

where λ_0 is the free-space wavelength. The physical length l of a microstrip line to yield a specified electrical length can be calculated from the following equations.

$$\beta l = \theta \tag{2.17}$$

since $$\frac{2\pi l}{\lambda_g} = \theta \tag{2.18}$$

The line length in terms of electrical angle in degrees is

$$l = \frac{\lambda_g \ \theta}{360} \tag{2.19}$$

Thus with λ_g evaluated using (1.8), the line length l can be found.

2.4 Modes of Propagation

Several field configurations, called modes of propagation, satisfy Maxwell's equations in the presence of transverse boundary conditions of the line. Every mode possesses its own propagation characteristics: attenuation and phase shift per unit length, propagation velocities, and cutoff frequency.

The various modes have different properties and they effectively distort the signal transmitted from the source. The different modes have different velocities and by selecting a low enough signal frequency, the line permits only one dominant mode to propagate. Thus multi-mode distortion can be prevented. The excitation of higher order modes sets an upper limit to the operating range of transmission lines. The dominant mode in a two-wire line has both its electric and magnetic fields transverse to the direction of propagation ($E_z=0$, $H_z=0$), and the

mode is called transverse electromagnetic (TEM). Any transmission line which is filled with a uniform dielectric can support a single, well-defined mode of propagation, at least over a specified range of frequencies (TEM for coaxial lines, TE_{10} for waveguides, etc). Transmission lines which do not have such a uniform dielectric filling cannot support a single mode of propagation; microstrip is within this category. Although the bulk of energy transmitted along the microstrip is with a field distribution which closely resembles TEM; it is usually referred to as 'quasi-TEM' [2]. There are three types of losses that occur in microstrip lines:

- Conductor (ohmic) losses in the strip conductor and ground plane.
- Dielectric losses in the substrate.
- Radiation losses.

2.5 Microstrip Dispersion

Frequency dispersion refers to the property of microwave transmission lines that have different group velocity versus frequency. When the frequency of a signal travelling on a microstrip line is doubled, the phase constant or wave number β ($= 2\pi/\lambda_g$) is not exactly doubled. Several transmission line structures exhibit this type of behavior, and this is applicable to non-TEM transmission lines such as microstrip and waveguides. Dispersion over a short bandwidth can often be ignored and becomes a problem in wide band width circuits transmitting for example a pulse.

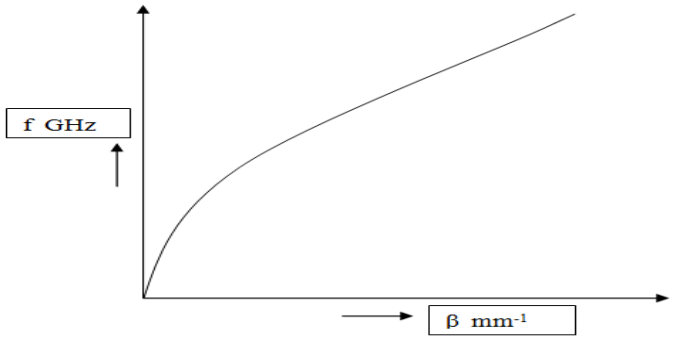

Figure 2.8 Dispersive effect in any general structure or system when frequency is plotted against phase constant.

Dispersion results from the effective dielectric constant, ε_{eff}, depending on frequency $\varepsilon_{eff}(f)$. The previous expressions for ε_{eff} are based on quasi-TEM approximations and are valid strictly at DC or at the lower microwave frequencies. Taking in to account of the frequency dependence $\varepsilon_{eff}(f)$ can be approximated as [4].

$$\varepsilon_{eff}(f) = \varepsilon_r - \frac{\varepsilon_r - \varepsilon_{eff}(f=0)}{1+P(f_n)} \tag{2.20}$$

$$P(f_n) = G(f/f_g)^2 \text{ and } f_g = \frac{Z_0(\varepsilon_{r,\ f=0})}{2\mu_0 h} \tag{2.21}$$

where, h is the substrate height and Z_0 is the characteristic impedance of the line under consideration. The coefficient G is an empirical parameter given as

$$G \approx 0.6 + 0.009 Z_0(\varepsilon_r)/\Omega \tag{2.22}$$

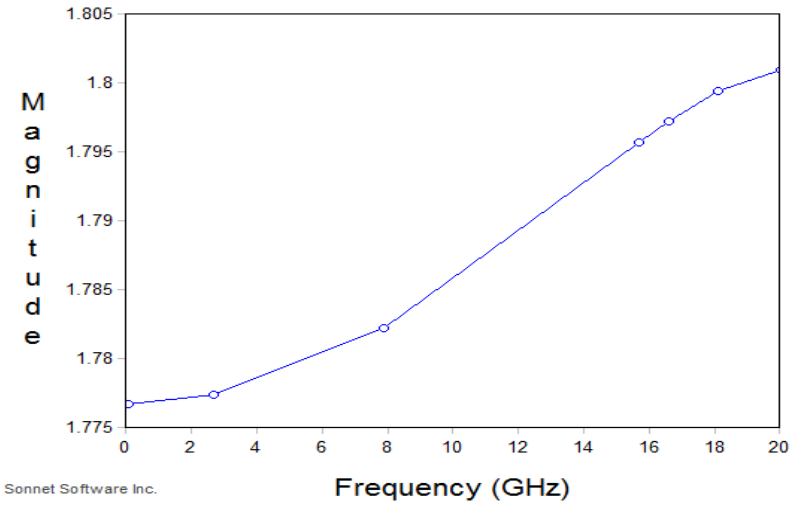

Figure 2.9 Variation of effective dielectric constant with frequency for $\boldsymbol{\varepsilon_r} = 1.96$.

As can be observed form the Figure 2.9, the value of effective dielectric permittivity ε_{eff} varies with frequency and it approaches ε_r as the frequency increases. The variation clearly shows that as frequency is increased, the wave is progressively slowed down. The limits of $\varepsilon_{eff}(f)$ can be now be seen, i.e.

$$\varepsilon_{eff}(f) \rightarrow \begin{cases} \varepsilon_{eff}, & f \rightarrow 0 \\ \varepsilon_r, & f \rightarrow \infty \end{cases} \tag{2.23}$$

Between these limits, $\varepsilon_{eff}(f)$ changes continuously with frequency.

2.7 Microstrip Simulations – open circuit and short circuit,

a) Consider an short circuited 75 Ω microstrip line on a substrate with permittivity $\varepsilon_r = 1.96$. The quarter wave electric length for the line at 8 GHz (center frequency) is 284 mils. The input impedance for this short circuit line is given by (1.22) as $Z_{in} = jZ_0 \tan \beta l$.

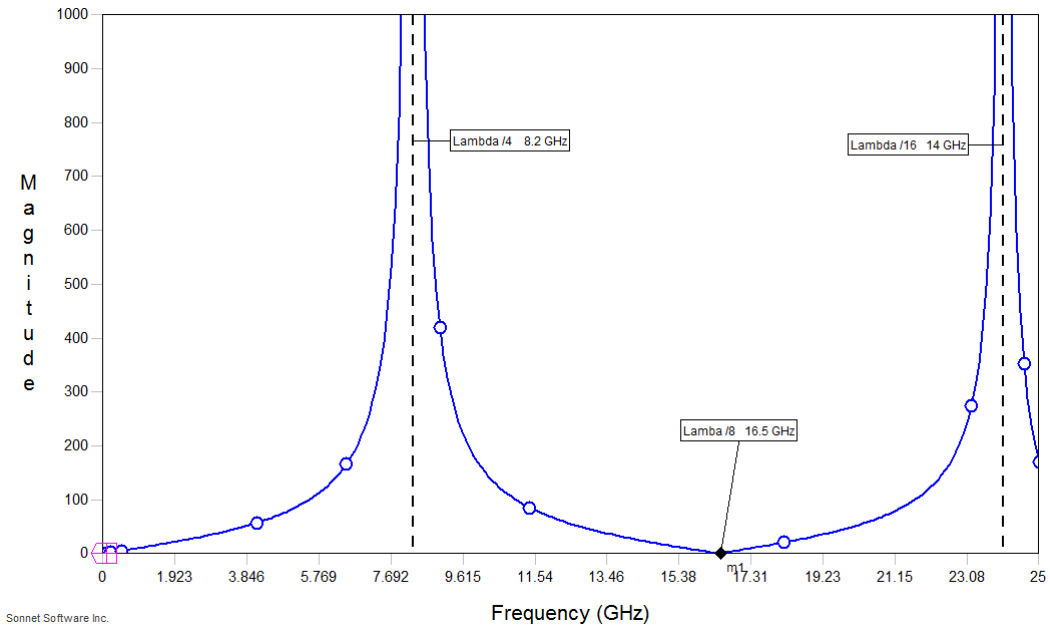

Figure 2.10 Variation of input impedance for a short-circuited microstrip line.

As can be observed from the Figure 2.10, the input impedance is inductive at the center frequency and it repeats for $\lambda/2$.

b) Consider the same line with the short replaced by an open-circuit. The input impedance for this open-circuit line is given as $Z_{in} = -jZ_0 \cot \beta l$. The simulated response of the input impedance is given in Figure 2.11. The input impedance can be observed to be capacitive at the center frequency (7.2 Ghz) and it repeats every $\lambda/2$.

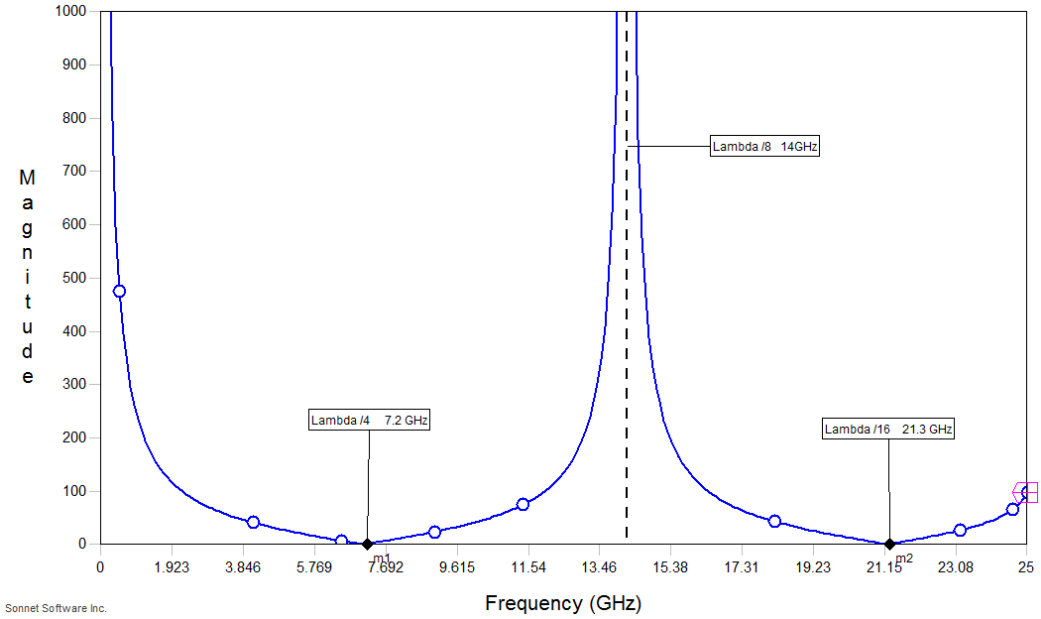

Figure 2.11 Variation of input impedance for open-circuited microstrip line.

It can be observed from Figure 2.10 and 2.11 that the frequency at which the line becomes a quarter wave length is different for the short-circuit and open-circuit cases. The two figures are combined and shown in Figure 2.12 for clarity.

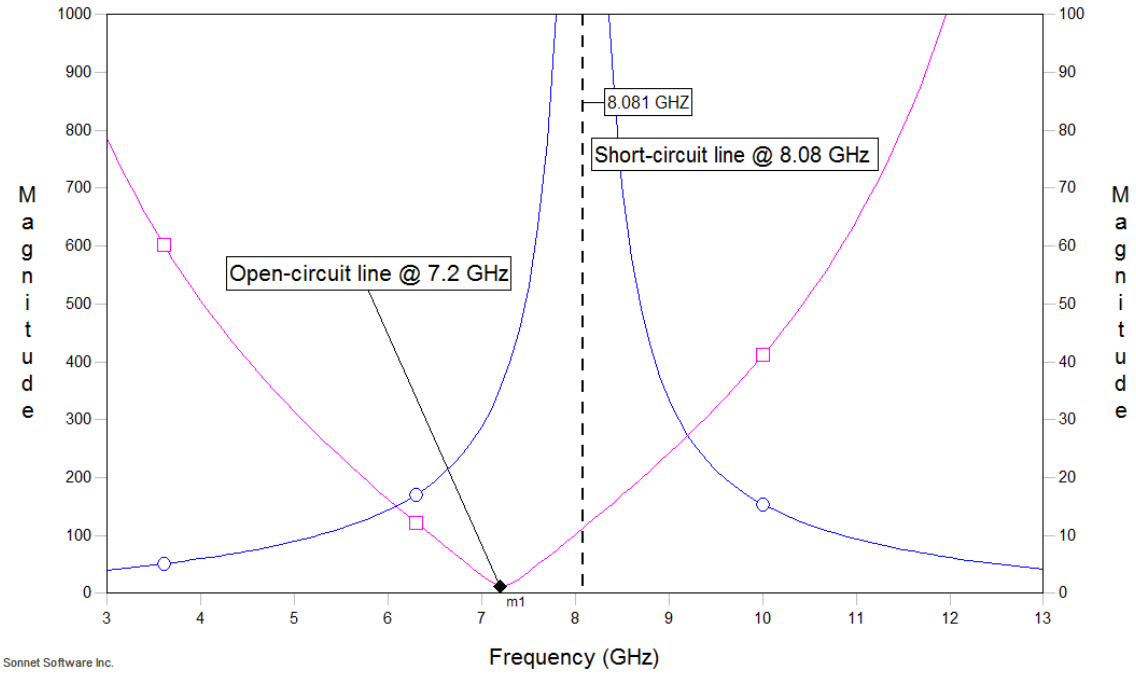

Figure 2.12 Simulation plot highlighting the open-end effect in microstrip.

This is due to open end-effect wherein the effective length of the line increases due to the presence of fringing fields which extent beyond the abrupt physical end of the metallic strip. This can be compensated by calculating the length of the extra length (l_{eo}) and compensating for this extra length. Several authors have given formulas for calculating the l_{eo}. The formula given by Edwards [2] is

$$l_{eo} \approx \frac{cZ_0C_f}{\sqrt{\varepsilon_{eff}}}, \tag{2.24}$$

where, C_f is the equivalent end fringing capacitance.

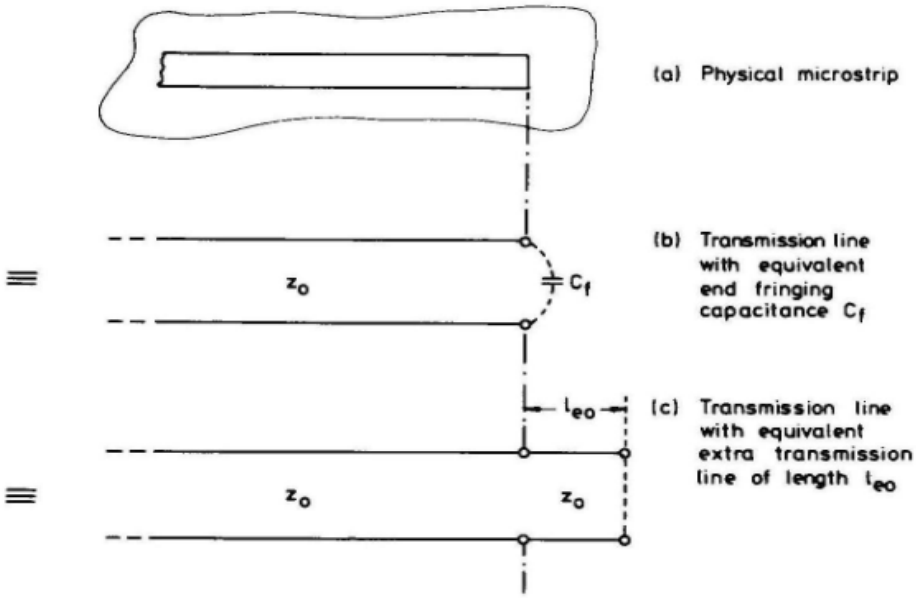

Figure 2.13 Equivalent end-effect length concept [2].

Another formula has been given by Hammerstad and Bekkadal [19] yielding the length directly.

$$l_{eo} = 0.412h\left(\frac{\varepsilon_{eff}+0.3}{\varepsilon_{eff}-0.258}\right)\left(\frac{W/h+0.262}{W/h+0.813}\right) \quad (2.25)$$

Equation (2.25) has been reported to give errors of 5% or more. Where such errors are acceptable, which is frequently the case, this should be used because it involves less computing than the more accurate (2.24).

CHAPTER 3

PLANAR COUPLED TRANSMISSION LINES

3.1 Introduction

Transmission lines used at microwave frequencies can be broadly divided into two categories: those that can support TEM (or quasi-TEM) mode of propagation and those that cannot. For TEM (or quasi-TEM) modes, the determination of important electrical characteristics (such as characteristic impedance and phase velocity) of single and coupled lines reduces to finding the capacitances associated with the structure.

3.2 Coupled Transmission Line

Two signals travelling along different transmission lines next to each other can be related to each other by assuming that both waves have a component that is common to both and a component that is different from each other. The common component is called the even and the differential component as odd. A simplest coupled line section can be represented as shown in Figure 3.1 [5]. Here, l is the length of the line, β is the phase constant and $Z_{0e}\ and\ Z_{0o}$ are the even and odd mode characteristic impedances of the line. The definitions of these impedances are given in section 3.4.

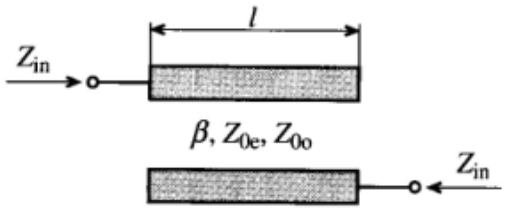

Figure 3.1 Transmission line representation of coupled line.

Consider two parallel strips, one at voltage V_1 and other at voltage V_2. Let the common voltage between the two be V_e, corresponding to the even mode and V_o corresponding to the odd mode. So,

$$V_1 = V_e + V_0 \tag{3.1}$$

$$V_2 = V_e + V_0 \tag{3.2}$$

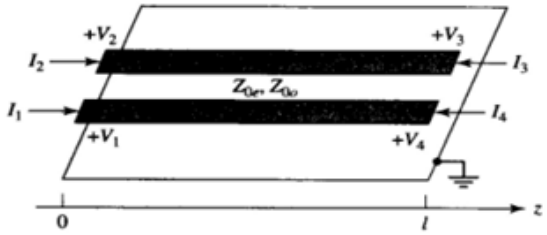

Figure 3.2 Parallel coupled section with voltage and current definitions [1].

Hence, the even and odd mode voltages are given by

$$V_e = \frac{V_1+V_2}{2} \tag{3.3}$$

$$V_o = \frac{V_1-V_2}{2} \tag{3.4}$$

This implies that there are two different characteristic impedance depending on whether the line is similarly excited or differentially excited. These impedances are called the even mode and odd mode characteristic impedances, Z_{oe} and Z_{0o} respectively. Also, due to the in-homogeneity in the microstrip, the velocities of propagation are different namely v_{pe} andv_{p0}. The electric and magnetic fields around a microstrip for even and odd mode excitation are shown in Figure 3.3 and 3.3 below [9]

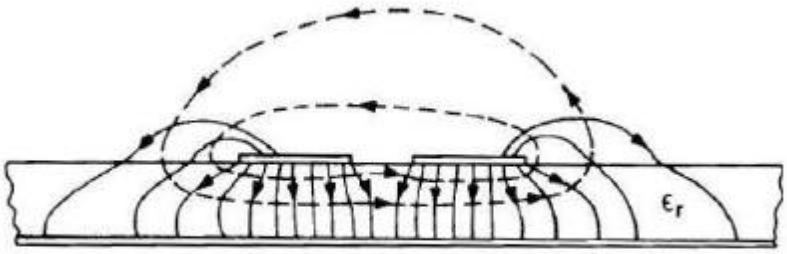

Figure 3.3 Electric and magnetic fields of a coupled microstrip line operating in even mode [9].

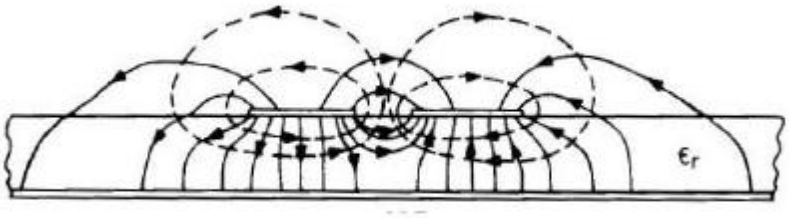

Figure 3.4 Electric and magnetic fields of a coupled microstrip line operating in odd mode [9].

3.4 Capacitance of Coupled Lines

The coupling between the lines can be expressed in terms of self and mutual capacitances. The Figure 3.5 below shows the cross section of two coupled transmission lines having a common ground conductor with the capacitances associated with the structure [10].

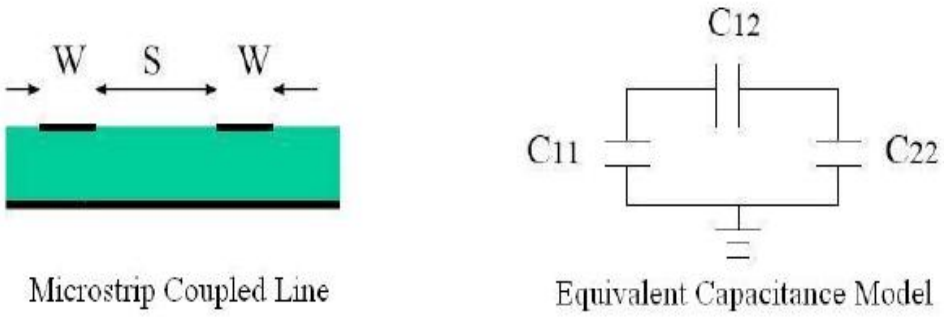

Figure 3.5 Microstrip coupled line and its equivalent capacitor model.

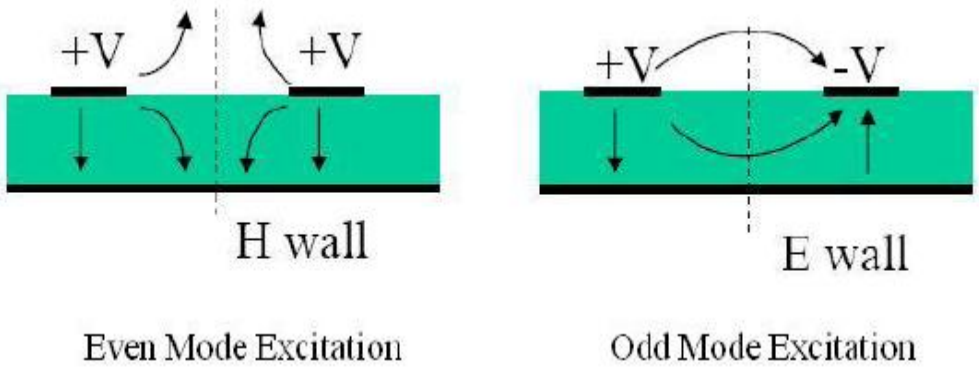

Figure 3.6 Even and odd modes of the coupled line with magnetic and electric wall symmetry.

The capacitance matrix of the two coupled transmission lines can be represented as

$$[C] = \begin{bmatrix} C_{11} & C_{12} \\ C_{21} & C_{22} \end{bmatrix} = \begin{bmatrix} C_a + C_m & -C_m \\ -C_m & C_b + C_m \end{bmatrix} \tag{3.5}$$

where C_{11} and C_{22} are the self-capacitances of lines 1 and 2 respectively in the presence of each other. C_a and C_b are the capacitance of line 1 and 2 with respect to ground respectively and C_m is the mutual capacitance between lines 1 and 2. The inductance matrix $[L]$ of a coupled line is given by [8]

$$[L] = \mu_0 \varepsilon_0 [C_0]^{-1} \tag{3.6}$$

where, μ_0, ε_0 are the free space permeability and permittivity respectively and $[C_0]$ denotes the capacitance matrix of the transmission lines obtained by assuming that these lines are placed in a medium of unity dielectric constant.

3.5 Empirical Formulae for Capacitance Calculation

Coupled line capacitance per unit length can be modeled by a system of three capacitors for each microstrip line. The three capacitances are the i) fringing field capacitance ii) parallel plate capacitance and iii) capacitance due to electric and magnetic wall symmetry. The analysis can be done separately for even and odd modes by taking in to account the effect of

electric and magnetic walls. The even and odd modes are shown in Figure 3.7 and Figure 3.8 respectively [2].

The expressions for the values of these capacitances are given by T. C. Edwards [2] after taking fringing fields into account. The parallel plate capacitance C_p and fringing capacitance C_f expressions are reproduced here as follows.

$$C_p = \frac{\varepsilon_r \varepsilon_0 W}{d} \tag{3.7}$$

$$C_f = \frac{\sqrt{\varepsilon_{eff}}}{2(cZ_0)} - \frac{C_p}{2} \tag{3.8}$$

where c is the speed of light through vacuum and Z_0 is the characteristic impedance of the coupled line under consideration.

The analysis uses the magnetic and electric walls at the line of symmetry (assuming equal width coupled lines) when even mode field and odd mode fields couple across.

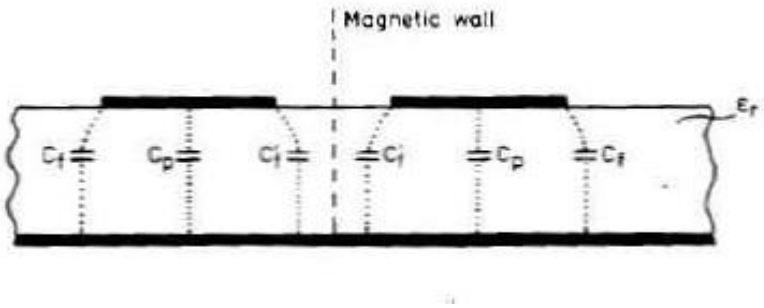

Figure 3.7 Model of a coupled line operating in even mode [2].

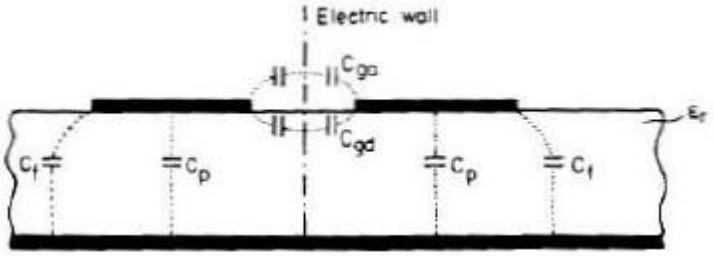

Figure 3.8 Model of a coupled line operating in odd mode [2].

The fringing capacitance $C_f^{'}$ with respect to the magnetic wall is given as [2]

$$C_f^{'} = \frac{C_f}{1+A(d/s)\tanh(8s/d)}\sqrt{\frac{\varepsilon_r}{\varepsilon_{eff}}}, \tag{3.9}$$

where

$$A = \exp\{-0.1\exp(2.33 - 2.53\ w/h)\}.$$

As can be observed from Figure 3.8 above, C_{ga} and C_{gd} represent, respectively air and dielectric odd mode fringing field capacitances across the coupling gap. Let

$$k = \frac{s/d}{(s/d+2(w/d))}$$

If $0 \leq k^2 \leq 0.5$, a term K is defined such that

$$K = \frac{1}{\pi}\ln\left(2\frac{1+(1-k^2)^{1/4}}{1-(1-k^2)^{1/4}}\right) \tag{3.10}$$

Else if $0.5 \leq k^2 \leq 1$,

$$K = \frac{\pi}{ln\{2(1+\sqrt{k})/(1-\sqrt{k})\}} \tag{3.11}$$

The capacitance with respect to the electric wall in air in terms of K is given as

$$C_{ga} = \varepsilon_0 K \tag{3.12}$$

The capacitance with respect to electric wall is given by

$$C_{gd} = \frac{\varepsilon_0\varepsilon_r}{\pi}\ln\coth\left(\frac{\pi s}{4h}\right) + 0.65C_f\left(\frac{0.02}{s/h}\sqrt{\varepsilon_r} + 1 - \varepsilon_r^{-2}\right) \tag{3.13}$$

Hence, the even and odd mode capacitances are given as

$$C_e = C_p + C_f + C_f', \tag{3.14}$$

$$C_o = C_p + C_f + C_{ga} + C_{gd}, \tag{3.15}$$

where C_p is the parallel plate capacitance with respect to the ground plane, C_f' the fringing field capacitance with respect to the magnetic wall (for even mode), C_{ga} and C_{ga} being the capacitances with respect to electric wall (for odd mode) in air and dielectric, respectively. C_f is the fringing capacitance.

The same capacitances are calculated for a strip suspended in air, i.e. for air as the substrate between the microstrip and ground. The effective dielectric constant ε_{eff} for this case is 1. The even and odd mode capacitances obtained with this ε_0 are C_{eair} and C_{oair}, respectively.

3.6 Calculation of Even-Odd mode Characteristic Impedances and Phase Velocities

The relationship between even and odd mode capacitances and impedances are given by

$$Z_{oe} = \frac{1}{v_{pe} C_e} = \frac{\omega}{\beta_e C_e} \tag{3.16}$$

and

$$Z_{oo} = \frac{1}{v_{po} C_o} = \frac{\omega}{\beta_o C_o} \tag{3.17}$$

where Z_{oe}, v_{pe}, β_e denotes the characteristic impedance, phase velocity and phase constant, respectively, of the even mode of the coupled lines; and Z_{oo}, v_{po}, β_o denote the same quantities for the odd mode. If the lines are placed in a homogenous medium of dielectric constant ε_r, the even and odd mode phase velocities are equal and are given by

$$v_{pe} = v_{po} = \frac{c}{\sqrt{\varepsilon_r}} \tag{3.18}$$

However, if the lines an placed in an inhomogeneous dielectric media (such as coupled microstrip lines), the even and odd mode phase velocities are, in general, different and are given by

$$v_{pe} = \frac{c}{\sqrt{\varepsilon_{ree}}} \tag{3.19}$$

and

$$v_{po} = \frac{c}{\sqrt{\varepsilon_{reo}}} \tag{3.20}$$

where ε_{ree} and ε_{reo} are defined as the even and odd-mode effective dielectric constants, respectively. These can be determined using

$$\varepsilon_{ree} = \frac{C_e}{C_{0e}} \tag{3.21}$$

and

$$\varepsilon_{reo} = \frac{C_o}{C_{0o}} \tag{3.22}$$

where C_{0e} and C_{0o} denote, respectively, the even- and odd mode capacitances of either line obtained by replacing the relative permittivity of the surrounding dielectric material by unity. C_e and C_o denote the corresponding capacitances in the presence of the inhomogeneous dielectric medium [8]. Using 3.14 to 3.18, equations 3.12 and 3.13 for even and odd mode characteristic impedances reduces to

$$Z_{0e} = \frac{1}{c\sqrt{C_e C_{0e}}} \tag{3.23}$$

$$Z_{0o} = \frac{1}{c\sqrt{C_o C_{0o}}} \tag{3.24}$$

3.7 Approximate Synthesis Technique

The equations for quasistatic characteristics of coupled microstrip lines have been given by many authors including Hammerstad and Jenson [16], Garg and Bahl [17], and others. Equations for the frequency dependence of the even and odd-mode effective dielectric

constants and characteristic impedances are given by Kirsching and Jansen [18]. It is observed that the variation of characteristic impedance with frequency is much smaller than the variation of effective dielectric constant. Also it is observed than even-mode parameters show a greater variation with frequency than odd-mode parameters.

3.8 Coupled Line Filters

Parallel coupled transmission line can also be used to construct many types of filters. Fabrication of multi-section band-pass or band-stop coupled line filters is particularly easy in microstrip or stripline form. Band width is usually limited by the difficulty in fabricating lines which are very close to each other. First the filter characteristics of a single quarter wave coupled line section are discussed. Other filter designs using coupled lines can be found in [13].

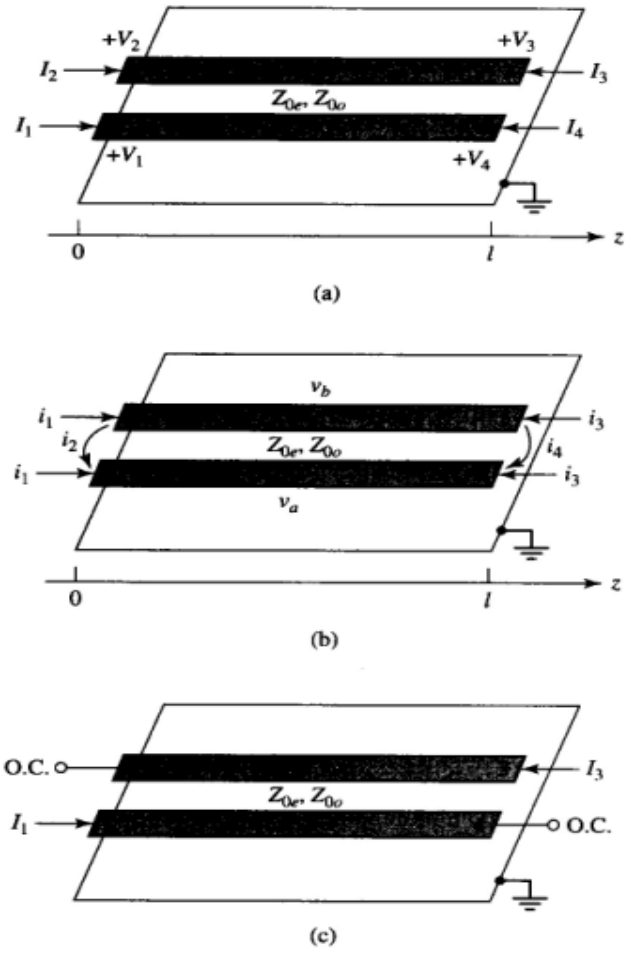

Figure 3.9 Defintions pertaining to a coupled line filter section. a) A parallel coupled section with port voltage and current definitions. b) A parallel coupled line section with even- and odd-mode current sources. c) A two port coupled line section having a bandpass response [1].

3.8.1 Analysis of a Single Coupled Section

A parallel coupled line section is shown in the Figure 3.9 above, with port voltages and current definitions. The open-circuit impedance matrix for this two port network is derived considering superposition of even- and odd- mode excitations [13]. The current sources i_1 and i_3 drive the line in the even mode, while i_2 and i_4 drive the line in the odd mode. By superposition, the total port current I_i can be expressed as [14].

$$I_1 = i_1 + i_2, \tag{3.25}$$

$$I_2 = i_1 - i_2, \tag{3.26}$$

$$I_3 = i_3 - i_4, \tag{3.27}$$

$$I_4 = i_3 + i_4 \tag{3.28}$$

Consider the line as being driven in the even mode by the i_1 current sources. If the other port is open circuited, the impedance seen at the port 1 or 2 is

$$Z_{in}^{e} = -j\, Z_{0e} \cot \beta l \tag{3.29}$$

The voltage on either conductor at $l = z$ can be expressed as

$$V_a^1(z) = V_b^1(z) = V_e^+\left[e^{-j\beta\,(z-l)} + e^{j\beta\,(z-l)}\right] \tag{3.30}$$

$$= 2V_e^+ cos\beta(l - z),$$

so the voltage at port 1 or 2 for $l = 0$ is

$$V_a^1(0) = V_b^1(0) = 2V_e^+ \cos \beta l = i_1 Z_{in}^{e}$$

This result and (3.29) can be used to rewrite (3.30) in terms of i_1 as

$$V_a^1(z) = V_b^1(z) = -jZ_{0e}\frac{cos\beta\,(l-z)}{sin\beta l} i_1 \tag{3.31}$$

Similarly, the voltage due to the current sources i_3 driving the line in the even mode are

$$V_a^3(z) = V_b^3(z) = -jZ_{0e}\frac{cos\beta z}{sin\beta l} i_3 \tag{3.32}$$

A similar analysis for odd mode currents yields,

$$V_a^2(z) = -V_b^2(z) = -jZ_{0o}\frac{cos\beta\,(l-z)}{sin\beta l} i_2 \tag{3.33}$$

$$V_a^4(z) = V_b^4(z) = -jZ_{0o}\frac{cos\beta z}{sin\beta l} i_4 \tag{3.34}$$

The total voltage at port 1 is

$$V_1 = v_a^1(0) + v_a^2(0) + v_a^3(0) + v_a^4(0)$$

$$= -j(Z_{0e} i_1 + Z_{0o} i_2)cot\theta - j(Z_{0e} i_3 + Z_{0o} i_4)csc\theta \tag{3.35}$$

where the results of (3.31), (3.32), (3.33), (3.34) were used and $\theta = \beta l$.

Next, solve for i_j in terms of *I s:*

$$i_1 = \frac{1}{2}(I_1 + I_2) \tag{3.36}$$

$$i_2 = \frac{1}{2}(I_1 - I_2) \tag{3.37}$$

$$i_3 = \frac{1}{2}(I_3 + I_4) \tag{3.38}$$

$$i_4 = \frac{1}{2}(I_4 - I_3) \tag{3.39}$$

substituting these in (3.35) gives,

$$V_1 = \frac{-j}{2}(Z_{0e}I_1 + Z_{0e}I_2 + Z_{0o}I_1 - Z_{0o}I_2)cot\theta$$

$$-\frac{j}{2}\,(Z_{0e}I_3 + Z_{0e}I_4 + Z_{0o}I_4 - Z_{0o}I_3)csc\theta \tag{3.40}$$

This result yields the top row of the open-circuit impedance matrix [Z] that describes the coupled line section. From the symmetry, all other matrix elements can be found once the first row is known. The matrix elements are

$$Z_{11} = Z_{22} = Z_{33} = Z_{44} = \frac{-j}{2}(Z_{0e} + Z_{0o})cot\theta, \tag{3.41}$$

$$Z_{12} = Z_{21} = Z_{34} = Z_{43} = \frac{-j}{2}(Z_{0e} - Z_{0o})cot\theta, \tag{3.42}$$

$$Z_{13} = Z_{31} = Z_{24} = Z_{42} = \frac{-j}{2}(Z_{0e} - Z_{0o})csc\theta, \tag{3.43}$$

$$Z_{14} = Z_{41} = Z_{23} = Z_{32} = \frac{-j}{2}(Z_{0e} + Z_{0o})csc\theta, \tag{3.44}$$

A two-port network can be formed from the coupled line section by terminating two of the four ports in either open or short circuits; there are ten possible combinations, as illustrated in the figure below, Pozar [1].

Circuit	Image Impedance	Response
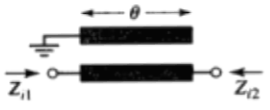	$Z_{i1} = \frac{2Z_{0e}Z_{0o}\cos\theta}{\sqrt{(Z_{0e}+Z_{0o})^2\cos^2\theta - (Z_{0e}-Z_{0o})^2}}$ $Z_{i2} = \frac{Z_{0e}Z_{0o}}{Z_{i1}}$	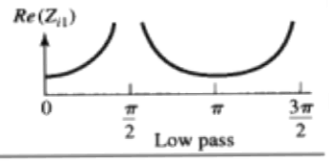
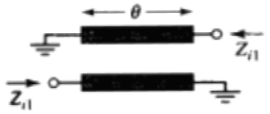	$Z_{i1} = \frac{2Z_{0e}Z_{0o}\sin\theta}{\sqrt{(Z_{0e}-Z_{0o})^2 - (Z_{0e}+Z_{0o})^2\cos^2\theta}}$	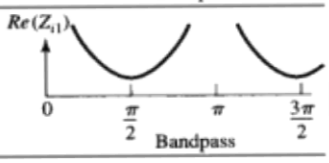
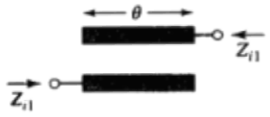	$Z_{i1} = \frac{\sqrt{(Z_{0e}-Z_{0o})^2 - (Z_{0e}+Z_{0o})^2\cos^2\theta}}{2\sin\theta}$	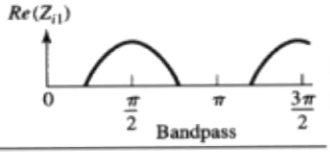
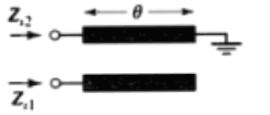	$Z_{i1} = \frac{\sqrt{Z_{0e}Z_{0o}}\sqrt{(Z_{0e}-Z_{0o})^2 - (Z_{0e}+Z_{0o})^2\cos^2\theta}}{(Z_{0e}+Z_{0o})\sin\theta}$ $Z_{i2} = \frac{Z_{0e}Z_{0o}}{Z_{i1}}$	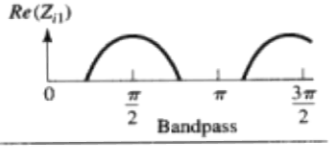
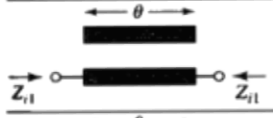	$Z_{i1} = \frac{Z_{0e}+Z_{0o}}{2}$	All pass
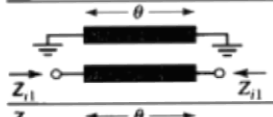	$Z_{i1} = \frac{2Z_{0e}Z_{0o}}{Z_{0e}+Z_{0o}}$	All pass
	$Z_{i1} = \sqrt{Z_{0e}Z_{0o}}$	All pass
	$Z_{i1} = -j\frac{2Z_{0e}Z_{0o}}{Z_{0e}+Z_{0o}}\cot\theta$ $Z_{i2} = \frac{Z_{0e}Z_{0o}}{Z_{i1}}$	All stop
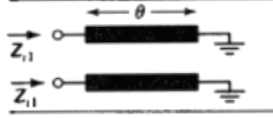	$Z_{i1} = j\sqrt{Z_{0e}Z_{0o}}\tan\theta$	All stop
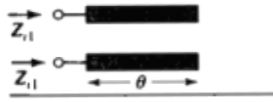	$Z_{i1} = -j\sqrt{Z_{0e}Z_{0o}}\cot\theta$	All stop

Figure 3.10 Ten Canonical coupled line circuits [1].

As indicated in Figure 3.10, the various circuits have different frequency responses, including low-pass, band-pass, all pass, and band stop. For band-pass filters, the third figure is most interesting, since open circuits are easier to fabricate than short circuits. In this case, $I_2 = I_4 = 0$, so the four port impedance matrix equations reduces to

$$V_1 = Z_{11}I_1 + Z_{13}I_3 \tag{3.45}$$

$$V_3 = Z_{31}I_1 + Z_{33}I_3 \tag{3.46}$$

where Z_{ij} is given in (3.41-3.44).

The filter characteristics can be analyzed by calculating the image impedance (which is the same at ports 1 and 3), and the propagation constant. The image impedance in terms of Z-parameters is

$$Z_i = \sqrt{Z_{11}^2 - \frac{Z_{11}Z_{13}^2}{Z_{33}}}$$

$$= \frac{1}{2}\sqrt{(Z_{0e} - Z_{0o})^2 csc^2\theta - (Z_{0e} + Z_{0o})^2 cot^2\theta} \tag{3.47}$$

when the coupled line is $\frac{\lambda}{4}$ long ($\theta = \pi/2$), the image impedance reduces to

$$Z_i = \frac{1}{2}(Z_{0e} - Z_{0o}), \tag{3.48}$$

which is real and positive, since $Z_{0e} > Z_{0o}$. When $\theta \to 0 \; or \; \pi, Z_i \to \pm j\infty$, indicating a stop band. The real part of the image impedance is shown in Figure 3.11 , where the cut off frequencies can be found from (3.47) as

$$cos\theta_1 = -cos\theta_2 = \frac{Z_{0e} - Z_{0o}}{Z_{0e} + Z_{0o}} \tag{3.49}$$

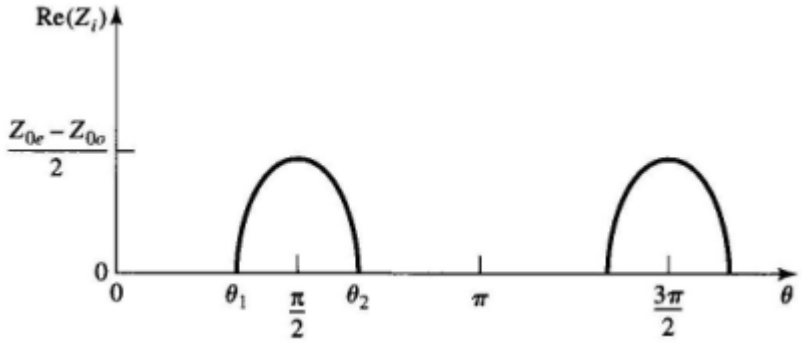

Figure 3.11 Real part of the image impedance of the band-pass network [5].

The propagation constant can be calculated as

$$\cos\beta = \sqrt{\frac{Z_{11}Z_{33}}{Z_{13}^2}} = \frac{Z_{11}}{Z_{13}} = \frac{Z_{0e}+Z_{0o}}{Z_{0e}-Z_{0o}}\cos\theta, \tag{3.50}$$

which shows β is real for $\theta_1 < \theta < \theta_2 = \pi - \theta_1$, where $cos\theta_1 = {(Z_{0e} - Z_{0o})}/{(Z_{0e} + Z_{0o})}$.

CHAPTER 4

MICROWAVE FILTER THEORY

4.1 Introduction

Filter design above a few GHz becomes difficult with discrete components since the wavelength starts to be comparable with the physical filter element dimensions, resulting in losses that limit its use. To arrive at practical filters, the lumped component filters must be converted in to distributed element realizations. To convert between lumped and distributed circuit designs, Richards proposed a special filter transformation that allows open and short transmission line segments to emulate the inductive and capacitive behavior of discrete components.

4.2 Richards Transformation

The application of modern network theory to the design of a microwave TEM distributed networks is based upon a complex plane transformation demonstrated by Richards in 1948. He showed that distributed networks, composed of commensurate lengths of transmission line and lumped resistors, could be treated in analysis or synthesis as lumped L-C-R networks by using the complex frequency variable $S= \sum + j\Omega$ and $\Omega = tan\ \frac{\pi\omega}{2\omega_0}$ where Ω is real and ω_0 is the radian frequency for which the transmission lines are quarter wavelength long. The tangent mapping function converts the range of frequencies $-\omega_0 \leq \omega \leq \omega_0$ in to the range $-\infty \leq \Omega \leq \infty$ and the mapping is repetitious in increments of $2\omega_0$. For example, the high-pass response of a lumped element filter in the frequency variable Ω maps in to band-pass response in ω about the quarter-wave frequency ω_0 for the corresponding distributed filter.

The input impedance of a short-circuited transmission line of characteristic impedance Z_0 is purely reactive [5]:

$$Zin = jZ_0 \tan(\beta l) = jZ_0 tan\theta \quad (4.1)$$

Here, the electrical length θ can be rewritten in such a way as to make the frequency behavior explicit. If we choose the line length to be λ/8 at a particular frequency $f_0=v_p/\lambda_0$, the electrical length becomes

$$\theta = \beta \frac{\lambda 0}{8} = \frac{2\pi f}{vp} \frac{vp}{8f0} = \frac{\pi f}{f0} = \frac{\pi \Omega}{4} \quad (4.2)$$

By substituting (4.2) in to (4.1), a direct link between the frequency dependent inductive behavior of the transmission line and the lumped element representation can be established.

$$jX_L = j\omega L = jZ_0 \tan\left(\frac{\pi f}{4f0}\right) = jZ_0 \tan\left(\frac{\pi}{4}\Omega\right) = SZ_0 \quad (4.3)$$

Where $S= jtan(\frac{\pi}{4}\Omega)$ is the actual Richards transform. The capacitive lumped element can be replicated through the open circuited transmission line section

$$jB_c = j\omega C = jY_0 \tan\left(\frac{\pi}{4}\Omega\right) = SY_0 \quad (4.4)$$

Thus, the Richards transformation allows us to replace lumped inductors with short-circuited stubs of characteristic impedance Z_0=L and capacitors with open-circuited stubs of characteristic impedance Z_0=1/C.

The Richards transformation maps the lumped element frequency response in the range $0 \le f \le \infty$ in to the range $0 \le f \le 2f_0$ due to the periodic behavior of the tangent function and the fact that all the lines are $\lambda_0/8$ (or $\lambda_0/4$) in length, a property known as commensurate line length. Because of this periodic property, the frequency response of such a filter cannot be regarded as broadband [5].

Richards theorem states that if the driving point impedance Z(S) is positive real and rational in S, then a unit element of value Z(1) may be extracted from the impedance function.

This leaves a factor of (S-1) in the numerator and denominator that cancels out, but does not reduce the order of the impedance function. If however, Z (1) = -Z (-1), then an added factor (S+1) also cancels from numerator and denominator. This does reduce the order of the impedance function. The non-redundant approximation problem is therefore to provide an impedance function Z(S) with Z (1) = =Z (-1) [3].

4.2.1 Distributed Capacitance and inductance

The input impedance of a short piece of open-circuited line is approximately

$$Z \approx \frac{Z_0}{j\omega\,(\frac{l}{v})} \tag{4.5}$$

So that its equivalent capacitance is

$$\text{C}= \frac{l}{vZ_0} = \frac{l\sqrt{\varepsilon r,eff}}{cZ_0} \tag{4.6}$$

Capacitance of about 1.3pF/cm with 50-Ω line on a general purpose PCB-FR4 can be expected. With relatively low-impedance lines, it might be practical to achieve roughly 4pF/cm. The capacitance limit diminishes quadratically as frequency increases because capacitance is proportional to area, which (in turn) is proportional to wavelength squared.

Similarly, the inductance of a short line terminated in a short circuit is given by

$$\text{L}= \frac{lZ_0}{v} = \frac{lZ_0\sqrt{\varepsilon r,eff}}{c} \tag{4.7}$$

A typical value for inductance is roughly on the order of 1nH/mm for the narrowest (highest impedance) practical lines in FR4. This approximate inductance limit is inversely proportional to frequency. To validate the approximations, we should therefore choose Z_0 as low as possible (or practical) to make a capacitor and choose Z_0 as high as possible to make an inductor [6].

Arbitrarily high characteristic impedance cannot be specified since there is always a lower bound on the width of the lines that can be fabricated reliably. There are also practical

bounds on the maximum width of the lines because all linear dimensions of a microstrip element must be comparable to the wavelength of interest to assure close approximation to lumped element behavior [6].

4.3 Unit Elements

When converting lumped elements in to transmission line sections, there is a need to separate the transmission line elements spatially to achieve practically realizable configurations. This is accomplished by inserting so-called unit elements (UEs). The unit element has an electrical length of $\theta = \frac{\pi}{4}(\frac{f}{f0})$ and characteristic impedance Z_{UE}. The two port network expression in ABCD parameter representation is:

$$[UE] = \begin{bmatrix} A_{UE} & B_{UE} \\ C_{UE} & D_{UE} \end{bmatrix} = \begin{bmatrix} cos\theta & jZ_{UE}sin\theta \\ \frac{jSin\theta}{Z_{UE}} & cos\theta \end{bmatrix} = \frac{1}{\sqrt{1-S^2}} \begin{bmatrix} 1 & Z_{UE}S \\ \frac{S}{Z_{UE}} & 1 \end{bmatrix}$$

where the definition of S is mentioned in section 4.2.

4.4 Kuroda' Identities

Kuroda's identities are used to convert a difficult to implement design to a more suitable filter realization. These identities are useful in making the implementation of Richard's transformation more practicable. They provide a list of equivalent two port networks that have precisely the same scattering matrices. In other words, using Kuroda's identities we can replace a two port network with its equivalent circuit and the behavior and characteristics of the circuit will not change. For example, a series inductance implemented by a short-circuited transmission line segment is more complicated to realize than a shunt stub line.

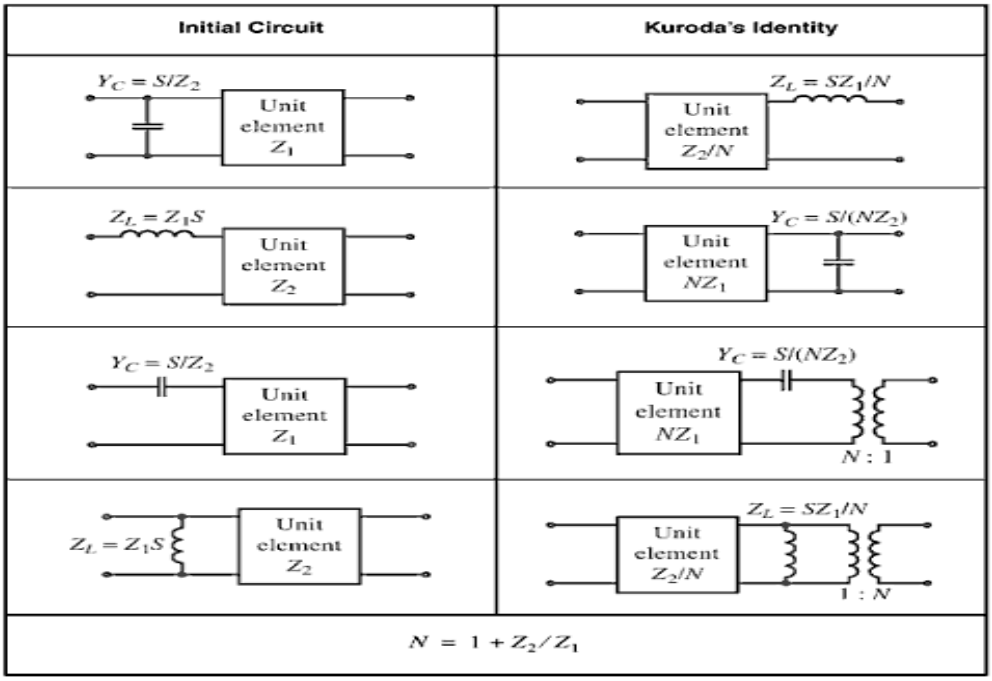

Figure 4.1 Kuroda's Identities [5].

In short, these identities can be used to:

- Physically separate transmission line stubs.
- Transform series stubs into shunt stubs.
- Change impractical characteristic impedance into more realizable ones.

4.5 Redundant Filter Synthesis

In general, redundant element filter synthesis proceeds as follows [2]:

- Select the filter order and parameters to meet design criteria.
- Replace the inductances and capacitances by equivalent λ/4 transmission lines.
- Convert series stub line into shunt stubs through Kuroda's identities.
- Denormalize and select equivalent microstrip lines (length, width and dielectric constant.).

4.6 Non-Redundant Filter

When synthesizing microwave filters, unit elements are used as part of the prototype circuit. The unit elements themselves will increase the number of poles of S_{21}, so they can be used to replace some of the inductors or capacitors of the lumped element prototype. In the extreme case, an nth order prototype circuit can be designed with no more than a total of n elements (including the unit elements in the count). This filter is called a non-redundant filter. This theory includes all microwave filter forms consisting entirely of quarter-wave lines, quarter-wave stubs, and coupled quarter-wave lines. A filter form termed the “optimum multipole” is obtained when each line length element characterized in the theory is used to create a complex plane pole to augment filter skirt response. Most conventional network forms are obtained from the optimum multipole form by introducing redundant elements. The method relies on extracting unit elements from the impedance function using Richard’s theorem rather than L’s and C’s. There is no analogous procedure in the theory of lumped circuit synthesis [3].

4.6.1 Design of Optimum Distributed Filters

The exact design of microwave TEM distributed filters based on modern network theory involves three distinct steps [7]:

1. Determination of the polynomial form of the ratio of reflection to transmission coefficient for a composite two-port filter containing both quarter-wave short or open circuit stubs (LC’s) and quarter-wave impedance transforming two ports (UE’s).
2. Development of the approximating function, usually chosen as maximally flat (Butterworth) or equal ripple (Chebyshev), used to approximate a rectangular low-pass or high-pas prototype power transmission characteristic.

3. Synthesis and physical realization of a practical network in the form of distributed quarter-wave lines.

Step 1 – Polynomial Ratio of the reflected to transmitted Power

The polynomial ratio of reflection to transmission coefficient for a cascade of unit elements and prototype unit elements can be obtained by multiplication of wave cascading matrices R [7] defined by

$$\begin{bmatrix} b_1 \\ a_1 \end{bmatrix} = \begin{bmatrix} r_{11} & r_{12} \\ r_{21} & r_{22} \end{bmatrix} \begin{bmatrix} a_2 \\ b_2 \end{bmatrix} \tag{4.8}$$

$$= \frac{1}{S_{21}} \begin{bmatrix} -\Delta s & S_{11} \\ -S_{22} & 1 \end{bmatrix} \begin{bmatrix} a_2 \\ b_2 \end{bmatrix} \tag{4.9}$$

In this, a_1, b_1 are the left-hand port incident and reflected wave amplitudes, respectively and a_2, b_2 are those of the right hand port. The R_{ij}'s are the R-matrix elements, the S_{ij}'s are the scattering matrix elements and $\Delta = S_{11}*S_{22}-S_{12}S_{21}$ is the scattering matrix determinant.

The R-matrix concept transforms the S-parameter representation to cascaded networks. In cascaded networks, it is more convenient to rewrite the power wave expressions arranged in terms of input and output ports. Cascading two-port networks is done by simple multiplication of r-matrices of individual two-ports. Thus, the chain scattering matrix plays a similar role as the ABCD-matrix discussed in Chapter 1. The R-matrix of distributed L's, C's and UE's are given in the Table 4.1. The constant matrix A in the Table 4.1 is defined by,

$A = \frac{1}{2}\begin{bmatrix} -1 & -1 \\ 1 & 1 \end{bmatrix}$ and I is the identity matrix. (4.10)

Table 4.1 Wave cascade matrix for distributed LC ladder and Unit elements.

Filter Type	Filter Elements	R-Matrix
Low -Pass	L	$Ls\left({}^{1}/_{Ls}\, I + \tilde{A}\right)$
	C	$Cs\left({}^{1}/_{Cs}\, I + A\right)$
	UE	$\frac{S}{\sqrt{1-S^2}}\left[\frac{1}{S} I + \left(Z\tilde{A} + Z^{-1}A\right)\right]$
High-Pass	UE	$\frac{1}{\sqrt{1-S^2}}\left[\left(Z\tilde{A} + Z^{-1}A\right)S + I\right]$
	C	$\frac{1}{CS}\left(CS\, I + \tilde{A}\right)$
	L	$\frac{1}{LS}\left(LS\, I + A\right)$

a) High-Pass Prototype

The high-pass response is shown in Figure 4.2 [7] gives. Such a distributed filter contains distributed series C's, shunt L's, UE's and a terminating load.

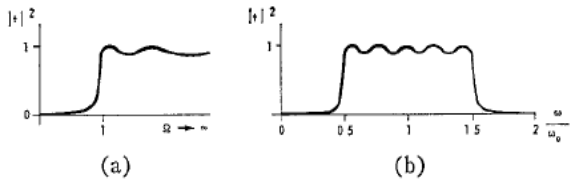

Figure 4.2 Mapping properties of the transformation$\Omega = \tan \pi\omega/2\omega_0$. a) Prototype lumped element high pass. b) Corresponding distributed element band-pass [7].

The C's, L's and UE's may occur in random sequence; however, in order to be a non-redundant filter, no two C's nor two L's may occur adjacent to each other even if separated by one or more UE's. It can be found from the r-matrix table above, each of the high-pass elements

has an R-matrix which has a scalar denominator factor multiplied by a matrix which is linear in the frequency parameter S. Thus an optimum high-pass filter, having a mixed cascade of m high-pas elements and n unit elements terminated in a unit load will have an overall R-matrix of the form

$$R = \left(\frac{1}{S}\right)^m \left(\frac{1}{\sqrt{1-S^2}}\right)^n B_{m+n}(S) \tag{4.11}$$

where $B_{m+n}(S)$ is an m+n degree 2x2 matrix polynomial in S.

$$B_{m+n}(S) = \begin{bmatrix} b_{11}(S) & b_{12}(S) \\ b_{21}(S) & b_{22}(S) \end{bmatrix}_{m+n} \tag{4.12}$$

The R-matrix of interest is $r_{12} = \frac{S_{11}}{S_{21}}$ representing the ratio of input reflected wave to that transmitted in to the load.

$$r_{12} = \frac{S11}{S21} = \left(\frac{1}{S}\right)^m \left(\frac{1}{\sqrt{1-S^2}}\right)^n b_{12\ m+n}(S) \tag{4.13}$$

Since the total power into the filter is conserved,

$$|\rho|^2 + |t|^2 = 1 \tag{4.14}$$

This can be rearranged to show that

$$|t|^2 = \frac{1}{1+\frac{|\rho|^2}{|t|^2}} = \frac{1}{1+|r_{12}|^2} \tag{4.17}$$

Equation 4.15 for $r_{12}(S)$ when multiplied by $r_{12}(-S)$ to give $|r_{12}|^2$ results in a ratio of (m+n)th degree polynomial in ($-S^2$). The general form of the resultant numerator, which has real coefficients, will not change if each term is multiplied by a real constant involving ${S_c}^2 = (j\ tan\theta_c)^2$, where $\theta_c = \frac{\pi\omega_c}{2\omega_0}$ and ω_c is designated to be the filter cutoff frequency. Then

$$\frac{|\rho|^2}{|t|^2} = \left(\frac{-S_c^2}{-S^2}\right)^m \left(\frac{1-S_c^2}{1-S^2}\right)^n P_{m+n}\left(\frac{-S^2}{-S_c^2}\right) \tag{4.15}$$

From the definition of S, we get S= $jtan\theta$. Substituting this in the above equation, we get

$$\frac{|\rho|^2}{|t|^2} = \left(\frac{tan\theta_c}{tan\theta}\right)^{2m} \left(\frac{cos\theta}{cos\,\theta_c}\right)^{2n} P_{m+n}\left(\frac{tan^2\theta}{\tan\,\theta_c}\right) \quad (4.16)$$

where P_{m+n} is an (m+n) th degree polynomial in $-S^2/-S_c^2$.

b) Low-Pas Prototype

The individual R-matrices of an optimum low-pass filter having m low pass ladder elements, n unit elements and a unit termination may be multiplied to obtain the overall R-matrix of the cascade. The low-pass optimum filter may be comprised of series L's, shunt C's and UE's in random sequence; however, to be non-redundant, L's must be adjacent to C's if not separated by a UE, or L's must be adjacent to each other (and likewise C's) if separated by a UE.

By applying a procedure similar to that used above for the high pass filter, the low-pass prototype response ratio of reflected to transmitted power is given by:

$$\frac{|\rho|^2}{|t|^2} = \left(\frac{-S^2}{-S_c^2}\right)^m \left(\frac{-S^2(1-S_c^2)}{-S_c^2(1-S^2)}\right)^n Q_{m+n}\left(\frac{-S_c^2}{-S^2}\right) \quad (4.17)$$

or by

$$\frac{|\rho|^2}{|t|^2} = \left(\frac{\tan\,\theta}{\tan\,\theta_c}\right)^{2m} \left(\frac{sin\theta}{sin\,\theta_c}\right)^{2n} Q_{m+n}\left(\frac{tan^2\theta_c}{\tan^2\theta}\right) \quad (4.18)$$

where Q_{m+n} is an (m+n) th degree polynomial in $-S_c^2/-S^2$.

Step 2 – Approximating functions

Two common approximations, which are considered here for application to the optimum multipole filter, are the maximally flat (Butterworth) and equal ripple (Chebyshev).

i) *Butterworth*: The maximally flat approximation for the high pass prototype results from choosing coefficients of the (m+n)th degree polynomial P_{m+n} (in equation 4.15) in a manner such that all but the highest order derivative of $\frac{|\rho|^2}{|t|^2}$, taken with respect to S^{-1} , are zero at S=0. The Butterworth approximation functions are then given by:

HP: $\frac{|\rho|^2}{|t|^2} = (\frac{S_c^2}{S^2})^{2m} \left(\frac{\sqrt{1-S_c^2}}{\sqrt{1-S^2}}\right)^{2n} = (\frac{tan\theta_c}{tan\theta})^{2m} \left(\frac{cos\theta}{cos\,\theta_c}\right)^{2n}$ (4.19)

LP: $\frac{|\rho|^2}{|t|^2} = (\frac{S^2}{S_c^2})^{2m} \left(\frac{S\sqrt{1-S_c^2}}{S_c\sqrt{1-S^2}}\right)^{2n} = (\frac{tan\theta}{tan\,\theta_c})^{2m} \left(\frac{sin\ \theta}{sin\ \theta_c}\right)^{2n}$ (4.20)

ii) *Chebyshev*: An equal ripple approximation for the high-pass prototype results from choosing coefficients of the polynomial, P_{m+n} in such a manner that the pass band response ripple varies between the values of unity and $(1+\varepsilon^2)^{-1}$. The detailed development of the polynomial form which exhibits this response is given in [7]. The Chebyshev approximating functions are given by:

HP: $\frac{|\rho|^2}{|t|^2} = \varepsilon^2 \left[T_m\left(\frac{S_c}{S}\right) T_n\left(\frac{\sqrt{1-S_c^2}}{\sqrt{1-S^2}}\right) - U_m\left(\frac{S_c}{S}\right) U_n\left(\frac{\sqrt{1-S_c^2}}{\sqrt{1-S^2}}\right)\right]^2$

$= \varepsilon^2 \left[T_m\left(\frac{tan\,\theta_c}{tan\theta}\right) T_n\left(\frac{cos\theta}{cos\,\theta_c}\right) - U_m\left(\frac{tan\,\theta_c}{tan\theta}\right) U_n\left(\frac{cos\theta}{cos\,\theta_c}\right)\right]^2$ (4.21)

LP: $\frac{|\rho|^2}{|t|^2} = \varepsilon^2 \left[T_m\left(\frac{S}{S_c}\right) T_n\left(\frac{S\sqrt{1-S_c^2}}{S_c\sqrt{1-S^2}}\right) - U_m\left(\frac{S}{S_c}\right) U_n\left(\frac{S\sqrt{1-S_c^2}}{S_c\sqrt{1-S^2}}\right)\right]^2$

$= \varepsilon^2 \left[T_m\left(\frac{tan\theta}{tan\,\theta_c}\right) T_n\left(\frac{sin\theta}{sin\,\theta_c}\right) - U_m\left(\frac{tan\theta}{tan\,\theta_c}\right) U_n\left(\frac{sin\theta}{sin\,\theta_c}\right)\right]^2$ (4.22)

where $T_m(x) = \cos(m\ arc\cos x)\ and\ U_m(x) = \sin(m\ arc\cos x)$ are the de-normalized m^{th} degree Chebyshev polynomials of first and second kind respectively.

Step 3 – Network Synthesis

The synthesis of a distributed network with a physical response correspondence to the admissible approximating function (4.19), (4.20) starts with finding the power reflection

coefficient $|\rho|^2$ from the approximating function for $\frac{|\rho|^2}{|t|^2}$ using the identity$|\rho|^2 + |t|^2 = 1$. After finding the reflection coefficient, the transformation $Zin = \frac{1+\rho}{1-\rho}$ yields the input impedance of one possible network and the opposite choice for algebraic sign of ρ gives the dual network. The choice of either network is dictated by the physical configuration of the desired realization and the element values obtained from the synthesis procedure. Richard's theorem can be applied to determine the unit element values, and pole removing techniques can be used to determine the LC values.

Consider a circuit in Figure 4.3 below which consists of a unit element with characteristic impedance Z_0 terminated with load Z_L. The input impedance is given by the transmission line equation.

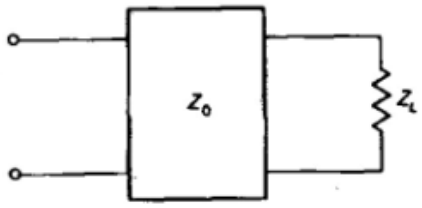

Figure 4.3 A unit element terminated in a load

$$\mathrm{Z(S)} = Z_0 \, \frac{Z_L(S)+Z_0 S}{Z_0+Z_L\,(S)S} \tag{4.23}$$

At S=1, the input impedance is equal to the characteristic impedance of the unit element.

$$\mathrm{Z(1)} = Z_0 \, \frac{Z_L(1)+Z_0}{Z_0+Z_L\,(1)} = Z_0 \tag{4.24}$$

Solving (4.23) for the load impedance Z_L(S) and substituting Z (1) =Z_0,

$$Z_L\,(S) = Z(1) \, \frac{Z(S)-SZ(1)}{Z(1)-SZ(S)} \tag{4.25}$$

Consequently, when a unit element of value Z (1) is extracted from the impedance function, the remainder is that given by (4.25). If Z (1) = -Z (-1), then the order of the remaining impedance function is reduced. Reduction of the impedance function continues by reapplication of Richard's theorem or by extraction of S-plane L's and C's whichever is appropriate.

CHAPTER 5

DESIGN OF BAND-PASS FILTER

5.1 Filter Realization

The final step in obtaining an optimum filter is solving the realization problem; i.e., it is desired to synthesize a distributed network that has a physical response corresponding to the requirement. Here a 5 pole, 0.2 dB ripple, 4-12 GHz band-pass filter is designed using the non-redundant method as discussed in Chapter 4.

5.1.1 Synthesis of the Input Impedance of the Network

The synthesis of the input impedance function starts with finding the reflection coefficient of the desired network. The power reflection coefficient $|\rho|^2 = 1 - |t|^2 = \rho\bar{\rho}$, where the bar denotes complex conjugate, can be obtained from the approximating function for $|\rho|^2/|t|^2$. Since the network has to be physically realizable, the reflection coefficient ρ must have no poles in the right half plane [7]. Once the reflection coefficient has been obtained by the above procedure, the transformation $Z_{in} = \frac{1+\rho}{1-\rho}$ yields the input impedance of one possible network and the opposite choice for the algebraic sign of ρ gives the input impedance of the dual of the network. Both the networks give identical response and the choice is dictated by the physical configuration of the realization and the element values obtained. From (4.21),

$$\frac{|\rho|^2}{|t|^2} = \varepsilon^2 \left[T_m\left(\frac{S_c}{S}\right) T_n\left(\frac{\sqrt{1-S_c^2}}{\sqrt{1-S^2}}\right) - U_m\left(\frac{S_c}{S}\right) U_n\left(\frac{\sqrt{1-S_c^2}}{\sqrt{1-S^2}}\right) \right]^2$$

Using the principle of conservation of energy, $|\rho|^2 + |t|^2 = 1$, $|t|^2$ can be found to be equal to

$$|t|^2 = \frac{1}{1+|\rho|^2/|t|^2}.$$

The transmission function is given by:

$$|t|^2 = \left\{1 + 0.047128\left[T_m\left(\frac{S_c}{S}\right)T_n\left(\frac{\sqrt{1-S_c^2}}{\sqrt{1-S^2}}\right) - U_m\left(\frac{S_c}{S}\right)U_n\left(\frac{\sqrt{1-S_c^2}}{\sqrt{1-S^2}}\right)\right]^2\right\}^{-2} \quad (5.1)$$

where, $T_m(x) = \cos(m\ arc\cos x)\ and\ U_m(x) = \sin(m\ arc\cos x)$ are the m[th] degree Chebyshev polynomial of the first and second kinds respectively.

Table 5.1 The Polynomials $T_m(x)$ and $U_m(x)$

m	$T_m(x)$	$U_m(x)$
0	1	0
1	x	$\sqrt{1-x^2}$
2	$2x^2-1$	$\sqrt{1-x^2}\,2x$
3	$4x^3-3x$	$\sqrt{1-x^2}\,(4x^2-1)$
4	$8x^4-8x^2+1$	$\sqrt{1-x^2}\,(8x^3-4x)$
5	$16x^5-20x^3+5x$	$\sqrt{1-x^2}\,(16x^4-12x^2+1)$

The number of unit elements 'n' is chosen as two and the number of high-pass elements 'm' as three. Equation (5.1) now becomes,

$$|t|^2 = \frac{1}{1+0.047128\left[T_3\left(\frac{S_c}{S}\right)T_2\left(\frac{\sqrt{1-S_c^2}}{\sqrt{1-S^2}}\right)-U_3\left(\frac{S_c}{S}\right)U_2\left(\frac{\sqrt{1-S_c^2}}{\sqrt{1-S^2}}\right)\right]^2} \quad (5.2)$$

Substitution of $S_c = j$, simplification of the resultant ratio of polynomials, and the use of the relation $|\rho|^2 + |t|^2 = 1$ gives:

$$\rho = \frac{0.48864\ S^4+0.14907\ S^2+0.8062}{S^5+3.94368\ S^4+6.23897\ S^3+6.49613\ S^2+3.37768\ S^1+1.71124} \quad (5.3)$$

For extracting a high-pass shunt inductance, Use the linear transformation $Y_{in} = \frac{1-\rho}{1+\rho}$ yields

$$Y_{in} = \frac{S^5+4.98034\ S^4+6.23897\ S^3+9.65879\ S^2+3.37768\ S+3.42248}{S^5+2.90701\ S^4+6.23897\ S^3+3.33347\ S^2+3.37768\ S+0.42478\,e-9} \quad (5.4)$$

The High-pass shunt inductance extracted from this function using synthetic division is found to be 0.98691. i.e, $Y_{in} = \left({}^1/_{Z_{in}{}'}\right) + {}^1/_{0.986S}$

The remaining input impedance function is:

$$Z_{in}{}' = \frac{S^4+2.90701\ S^3+6.23897\ S^2+3.33347\ S+3.37768}{S^4+3.96707\ S^3+3.29339\ S^2+3.33707\ S} \quad (5.5)$$

The function is checked for the presence of a Unit Element (U.E). The condition to be satisfied is:

$$Z_{in}{}'(1) = -Z_{in}{}'(-1)$$

$Z_{in}{}'(1)$ is found to be 1.45351 and $Z_{in}{}'(-1) = -1.45351$ i.e, $Z_{in}{}'(1) = -Z_{in}{}'(-1)$ and the condition for the existence of unit element is satisfied. The value of the normalized unit element is 1.45351. The impedance of the remaining network after the removal of unit element is:

$$Z_{in}^{''}(S) = Z_{in}^{'}(1)\ \frac{Z_{in}^{'}(S) - SZ_{in}^{'}(1)}{Z_{in}^{'}(1) - SZ_{in}^{'}(S)} \tag{5.6}$$

$$Y_{in}^{''}(S) = 1/Z_{in}^{''}(S) = \frac{-S^3 - 1.45350\ S^2 - 1.47278\ S + 0.39793e-10}{-2.11268\ S^3 - 6.92769\ S^2 - 4.84523\ S - 4.90949} \tag{5.7}$$

A high-pass series capacitor of value 0.29998 is extracted from this function by synthetic division, and the remainder function is:

$$Y_{in}^{'''}(S) = \frac{-S^2 - 1.45350\ S - 1.47278}{-2.11268\ S^2 - 3.59421\ S} \tag{5.8}$$

$Y_{in}^{'''}(S)$ is checked for presence of unit elements, and a UE of value 1.45351 is extracted. The impedance of the remaining network is:

$$Z_{in}^{''''}(S) = \frac{S - 0.71933e-10}{S + 1.01326} \tag{5.9}$$

By doing synthetic division as performed previously, a high pass shunt inductance of value 0.98691 is extracted. This completes the division process and we have all the element values now. The extracted element values after de-normalizing to Z_0 are:

Table 5.2 De-Normalized Element Values Computed

Element-1	Shunt Inductance (shorted Stub Z0)	49.3
Element-2	Unit Element Z0	72.6
Element-3	Series Capacitance (Open Stub Z0)	166.
Element-4	Unit Element Z0	72.6
Element-5	Shunt Inductance (shorted Stub Z0)	49.3

The above computed values are simulated in Agilent-ADS to verify the performance. The schematic and results of the simulation are given below in Figure 5.1 and 3.17 respectively.

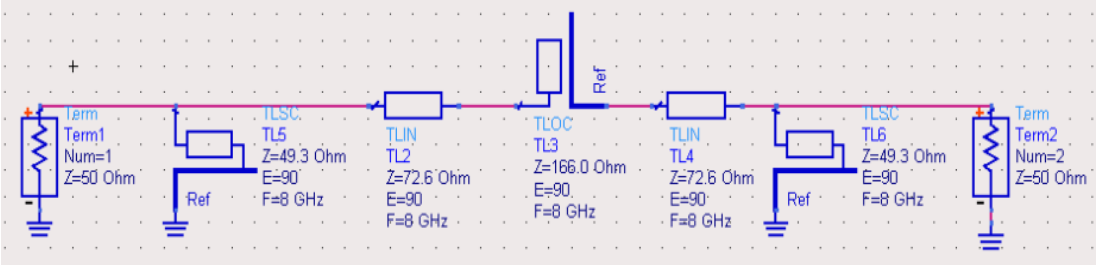

Figure 5.1 ADS Schematic of the proposed filter

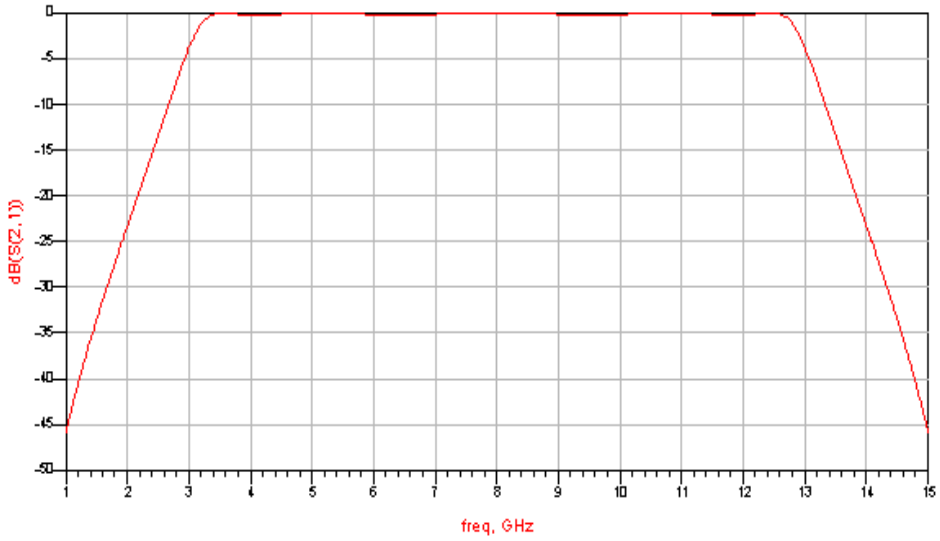

Figure 5.2 S21 of the simulated filter in ADS.

5.1.2 Synthesis of the quarter-wave Transmission lines

To realize the filter with practical transmission line circuits, *ADS-LINECALC* was used to find the transmission line parameters. The parameters for the 49 Ω and 73 Ω lines were found to be as mentioned in Table 5.3 below for Rogers5880-LZ 60mil board with ε_r of 1.96.

Table 5.3 Transmission Line Parameters

Element	Z_0 (Ω)	W (mils)	L (mils)
Shunt Inductance	49	210	280
UE	73	110	280
Series Capacitor	166	--	--

The series capacitive element of characteristic impedance 166 Ω poses a challenge to design and fabricate using microstrip since series stubs are not possible with printed circuit boards.

5.1.3 Investigation of Different Possible Configurations for Series Stub

To achieve the high characteristic impedance of the series element, a parallel plate transmission line was considered, since it is possible to achieve the high impedance with reasonable line widths. Details of the problems in using this structure as series elements are outlined in the next section. Since this method did not prove to be successful, a coupled line approach is tried and found to be suitable for the present application. However the coupling gap was found to be at the lower limit of lab fabrication limits. Still this approach was tried out and was successful in fabricating the board.

a) Double Sided Parallel Transmission Line

A double sided parallel-strip is a balanced line, as shown in Figure 5.3. For the same strip width, the characteristic impedance of a double-sided parallel-strip line with dielectric separation *h* is twice the characteristic impedance of a microstrip line with dielectric thickness *t*=*h*/2 [15]. The effective dielectric constant remains the same in this situation [20]. As an

example, a 50 Ω line on a printed circuit laminate with ε_r=10.2 and dielectric height of 25 mils will have a width of 37 mills on a double-sided parallel strip and 22 mills on a microstrip.

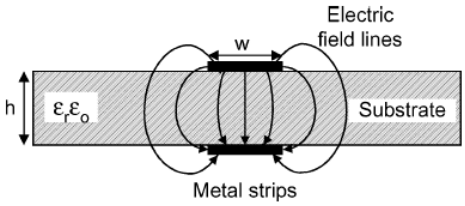

Figure 5.3 Cross Section of double-sided parallel-strip transmission line [15].

The characteristic impedance of paired transmission lines is given by [21], [22] as

For wide strips $\left({}^{a}/_{b} > 1\right)$, where $a = \frac{w}{2}$ and $b = h/2$:

$$Z_0 = \frac{\eta_0}{\sqrt{\varepsilon_r}}\left\{\frac{a}{b} + \frac{1}{\pi} ln4 + \frac{\varepsilon_r+1}{2\pi\varepsilon_r} ln\left[\frac{\pi\varepsilon\,(a/b+0.94)}{2}\right] + \frac{\varepsilon_r-1}{2\pi\varepsilon_r^2} ln\frac{\varepsilon\pi^2}{16}\right\}^{-1} \Omega \qquad (5.10)$$

For wide strips $\left({}^{a}/_{b} < 1\right)$,

$$Z_0 = \frac{\eta_0}{\pi\sqrt{\varepsilon_r}}\left[ln\frac{4b}{a} + \frac{1}{8}\left(\frac{a}{b}\right)^2 - \frac{\varepsilon_r-1}{2(\varepsilon_r+1)}\left(ln\frac{\pi}{2} + \frac{ln\,{}^{4}/_{\pi}}{\varepsilon_r}\right)\right] \Omega \qquad (5.11)$$

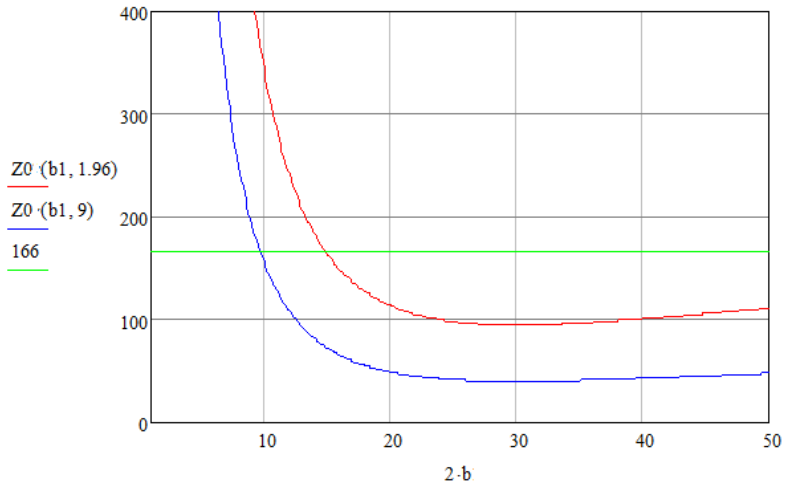

Figure 5.4 Variation of Characteristic impedance of double sided parallel strip line with varying board thickness 'h=2b' and fixed width 'w'.

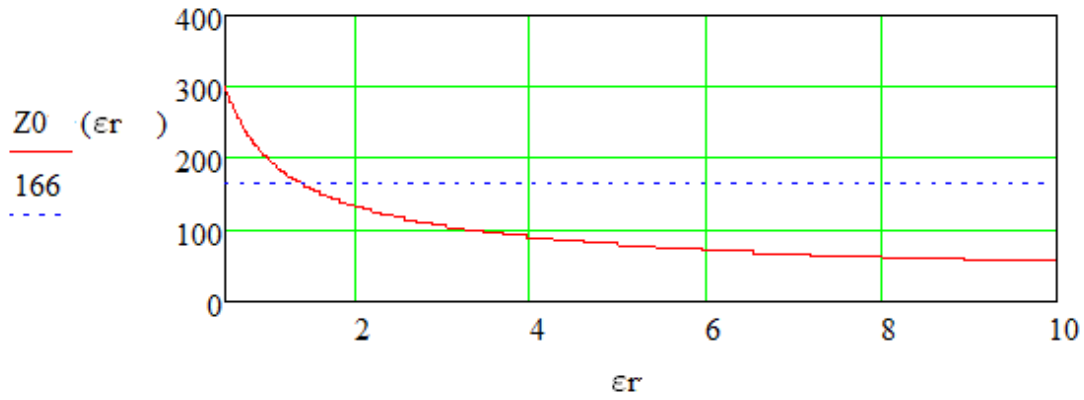

Figure 5.5 Variation of characteristic impedance of double sided parallel strip line with fixed dimensions and varying ε_r.

A transmission line form of the series stub is shown in Figure 5.6 below. With $l_s = \lambda/4$, at the design frequency, the input impedance of the open-circuited stub is zero and hence the microwave signal passes unattenuated to the output port. Given a source and load with impedance Z_0 and a series stub with characteristic impedance Z_{os},

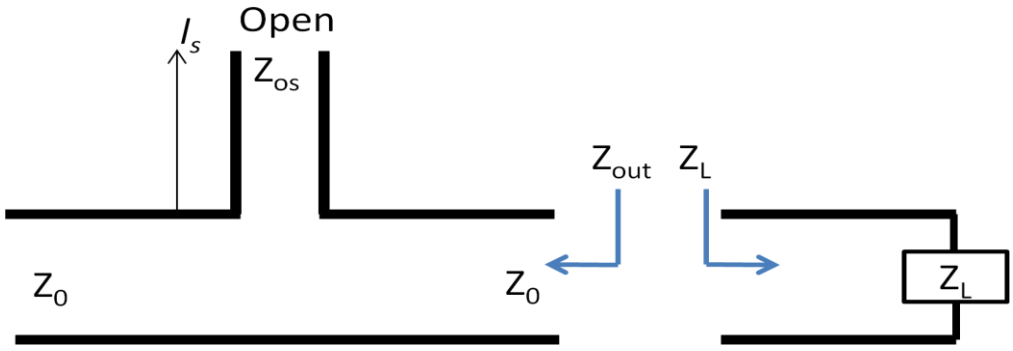

Figure 5.6 Transmission line series stub.

The VSWR of the line can be calculated as

$$VSWR = \frac{1 + \rho(S)}{1 - \rho(S)}$$ Where, ρ is the reflection coefficient.

$$\rho = {Z_{out}(S) - Z_L}\Big/{Z_{out}(S) + Z_L}$$

where, Z_L is the load impedance and Z_0 is the source impedance. Substituting this in the equation for VSWR, we get $VSWR = {Z_L}/{Z_0}$.

For the circuit in Figure 5.6, $\overline{Z_{in}} = Z_0 - jZ_{os}cot\left({2\pi l_s}/{\lambda}\right)$, which is also the input impedance of the circuit.

Hence,

$$VSWR = 1 - j\left({Z_{os}}/{Z_0}\right)cot\left({2\pi l_s}/{\lambda}\right)$$

and

$$\overline{Z_{in}} = 1 - j\left({Z_{os}}/{Z_0}\right)cot\left({2\pi l_s}/{\lambda}\right)$$

With $l_s = \lambda/4$ at the center frequency, $\overline{Z_{in}} = 1\ and\ VSWR = 1$. This $VSWR$ is higher at other frequencies since the $cot\left({2\pi l_s}/{\lambda}\right)$ term is no longer zero. To minimize this effect and hence broadband the microwave performance, Z_{os} should be as small as possible.

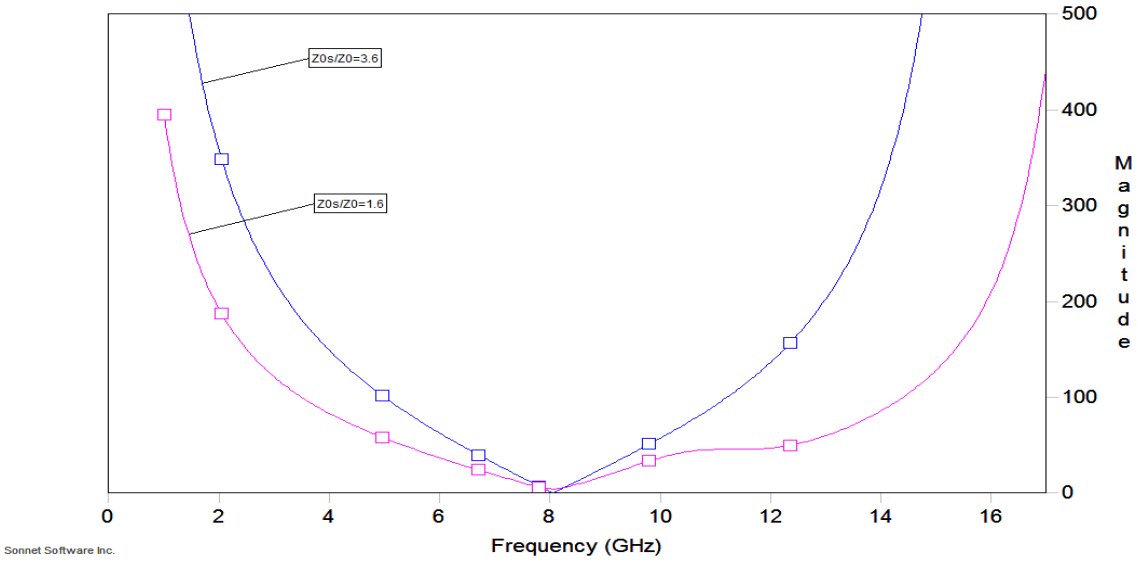

Figure 5.7 Variation of input impedance for two open circuit series stub parallel transmission lines having characteristic impedance of 180Ω and 80Ω (Reference impedance Z_0= 50Ω).

Thus with the series stub of impedance 166 Ω, an open circuit parallel strip will have very narrow band response which will not be suitable for the present problem. Hence this approach was ruled out. To verify this, two series stubs of characteristic impedance 180 Ω and 80 Ω were simulated in Sonnet. As shown in Figure 5.7, the input impedance is purely capacitive only at one frequency for both the lines, but the 80 Ω line has a broader response indicating wider bandwidth.

b) Coupled Line Band-Pass Filter

A filter using coupled lines is designed for simulating the band-pass characteristic of the series capacitor. The design formulas are mentioned in section 3.8.1. It is desired to have a pass band at least from 6 to 11 GHz to get a median frequency of 8 GHz (center frequency). As given in section 3.8.1, the band edges are defined by

$$cos\theta_1 = -cos\theta_2 = \frac{Z_{0e}-Z_{0o}}{Z_{0e}+Z_{0o}} \quad (5.12)$$

and θ_1 is computed from $\theta_1 = \frac{360\ l\sqrt{\varepsilon_{eff}}}{\lambda_0}$

Using an effective dielectric constant of 1.6, θ_1 and θ_2 are calculated to be $62.75^0\ and\ 115^0$ respectively. Using this in (5.12), the ratio of Z_{0e} to Z_{0o} is found

$$Z_{0e}/Z_{0o} = 2.69 \tag{5.13}$$

Using the relation $Z_0 = \sqrt{Z_{0e} \times Z_{0o}}$, and assuming Z_{0o} to be 105 Ω, Z_{0e} can be found to be 262 Ω. Synthesis formulas given in Chapter 3 can be used to find the coupler dimensions for the given value of Z_{0e} and Z_{0o} Rogers 5880LZ 60 mil thick board with ε_r =1.96 was used. The microstrip dimensions were found to be

$$\frac{W}{h} = 0.172 \text{ and } \frac{s}{h} = 0.216$$

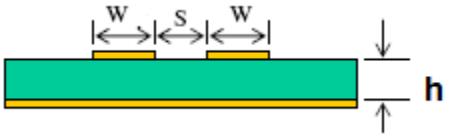

Figure 5.8 Definition of coupled line parameters.

Since h is known to be 60 mils, *W* and s can be calculated. Calculated values of *W* and s are

$$W \approx 10 \text{ mills } s \approx 12.96 \text{ mills}$$

A corresponding structure is laid out using the program Sonnet and simulated. Sonnet provides electromagnetic modeling of all layout details including parasitic, cross coupling, enclosure and package resonance effects. The software requires a physical description of the circuit (layout and material properties) and employs rigorous Method-of-Moments analysis to calculate S, Y, Z or extracted SPICE models. The schematic is of the structure and the simulated results are shown in Figure 5.9 and 5.10 respectively.

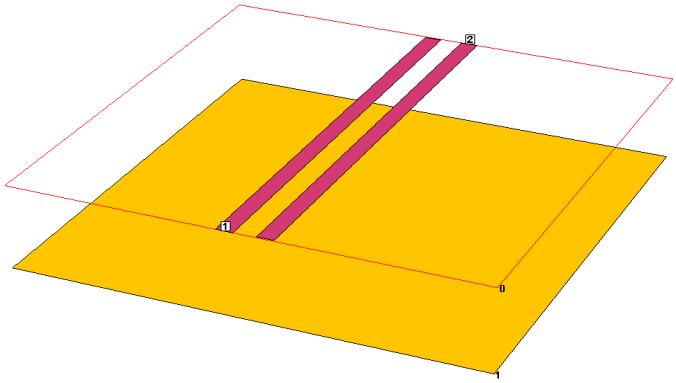

Figure 5.9 Sonnet Layout of coupled line filter

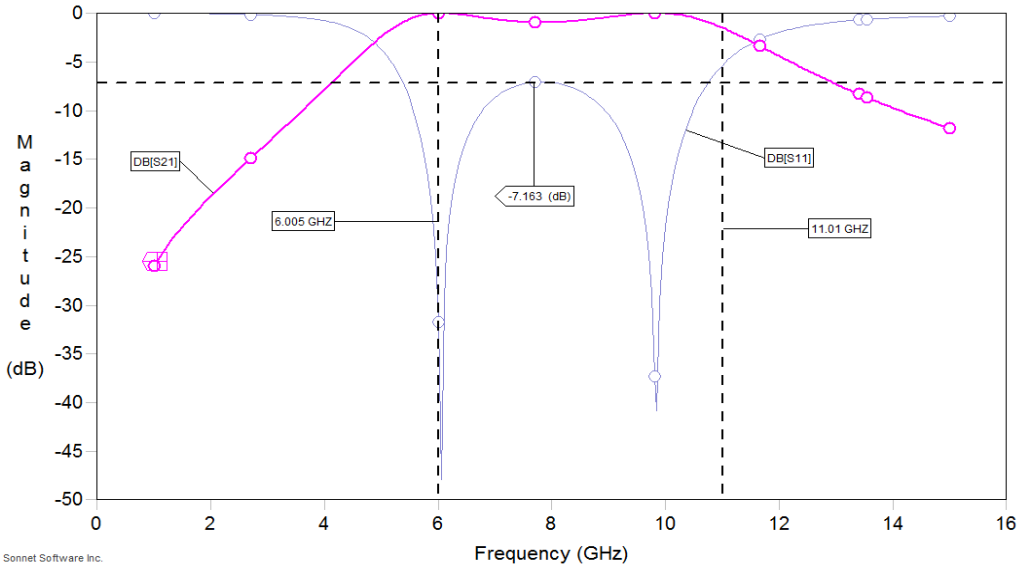

Figure 5.10 Simulated results for the coupled line filter.

The final layout of the filter is done in *sonnet* using the element values computed before and the series bandpass structure designed above. The layout is further optimized using the optimization tool in sonnet to give a better filter response. The layout and the simulated filter response curves are given in Figure 5.11 and Figure 5.13 respectively.

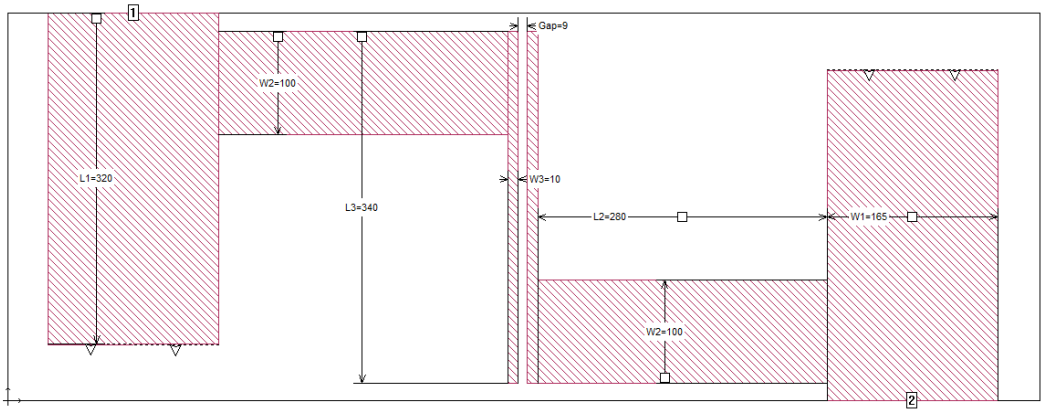

Figure 5.11 Layout of the filter (ε_r=1.96, h=60 mil)

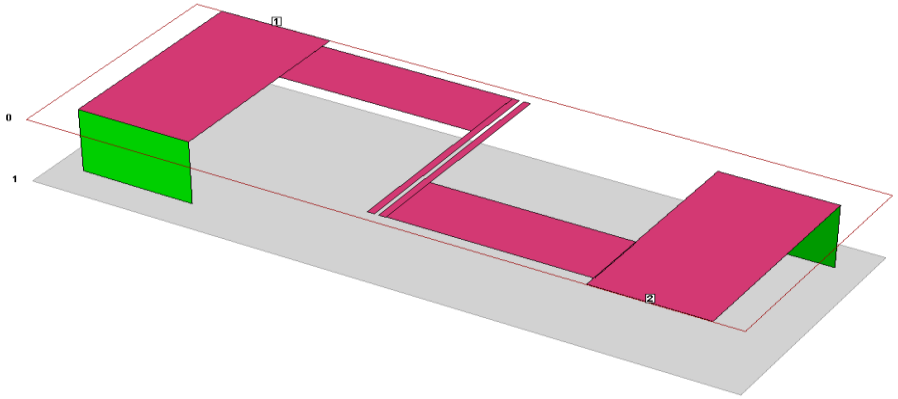

Figure 5.12 3D view of the final filter.

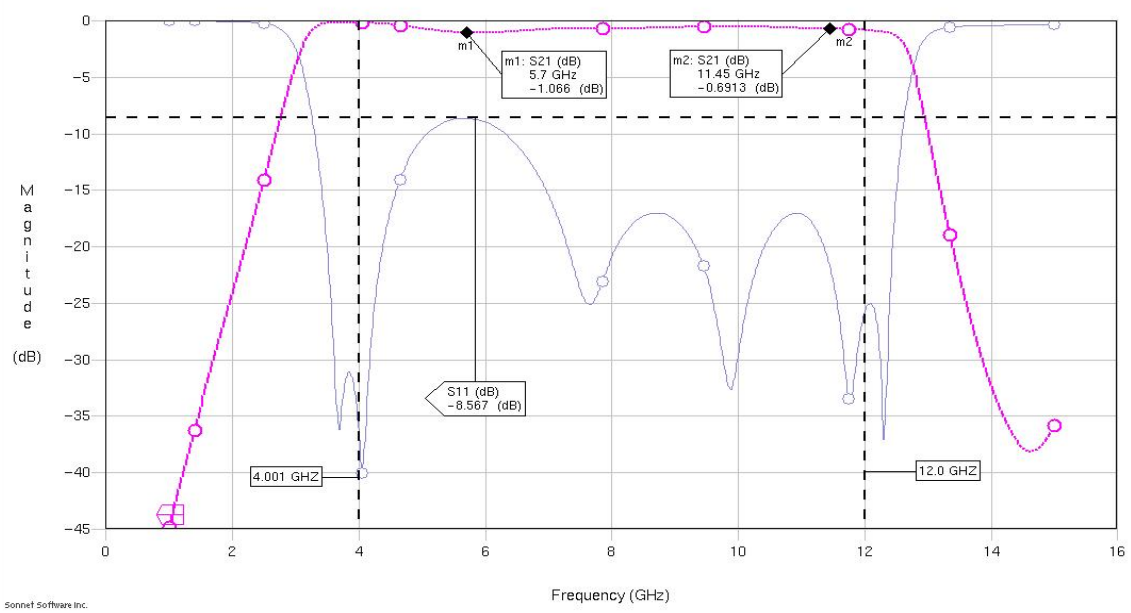

Figure 5.13 S_{21} and S_{11} of the filter from sonnet simulation.

5.1.4 Group Delay

Group delay response of the filter is shown in Figure 5.14. The delay response shows a variation from 0.1559 ns to 0.3226 ns over the pass band.

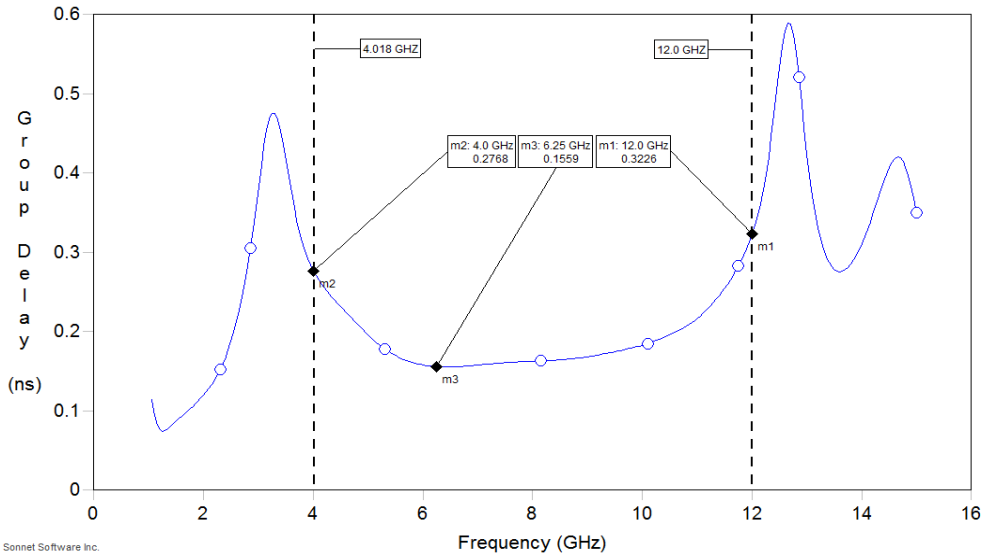

Figure 5.14 Group delay response

5.1.5 Fabrication of the Filter

The layout of the filter was done on Eagle Layout Editor, and was transferred to inkjet paper from staples. After preparing the copper board, an electric iron is used to transfer the image to the board to create the 'mask'. The board along with the mask is left to soak in water for around 1 hour after which the back-paper can be peeled off. The board is then etched using ferric chloride solution and cleaned using acetone. The board is then cut to the correct size and inspected for any short between the coupled lines. Finally the shorting of stubs and terminal connectors are installed. The photograph of the fabricated filter is shown in Figure 5.15. However, in the actual measured filter the microstrip launcher were placed even with the stub so there was no air gap between the launcher face and the beginning of the filter stub.

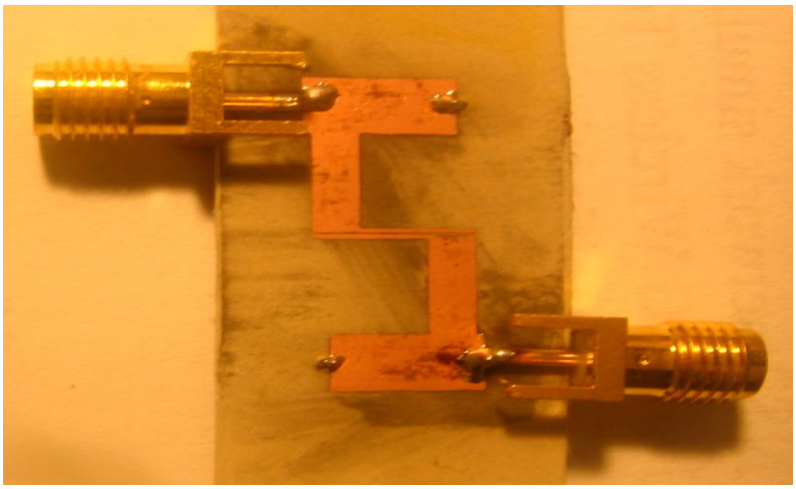

Figure 5.15 Photograph of the fabricated board.

5.2 Test Results

The fabricated filter is tested using a vector network analyzer and the initial results are as shown in Figure 5.16.

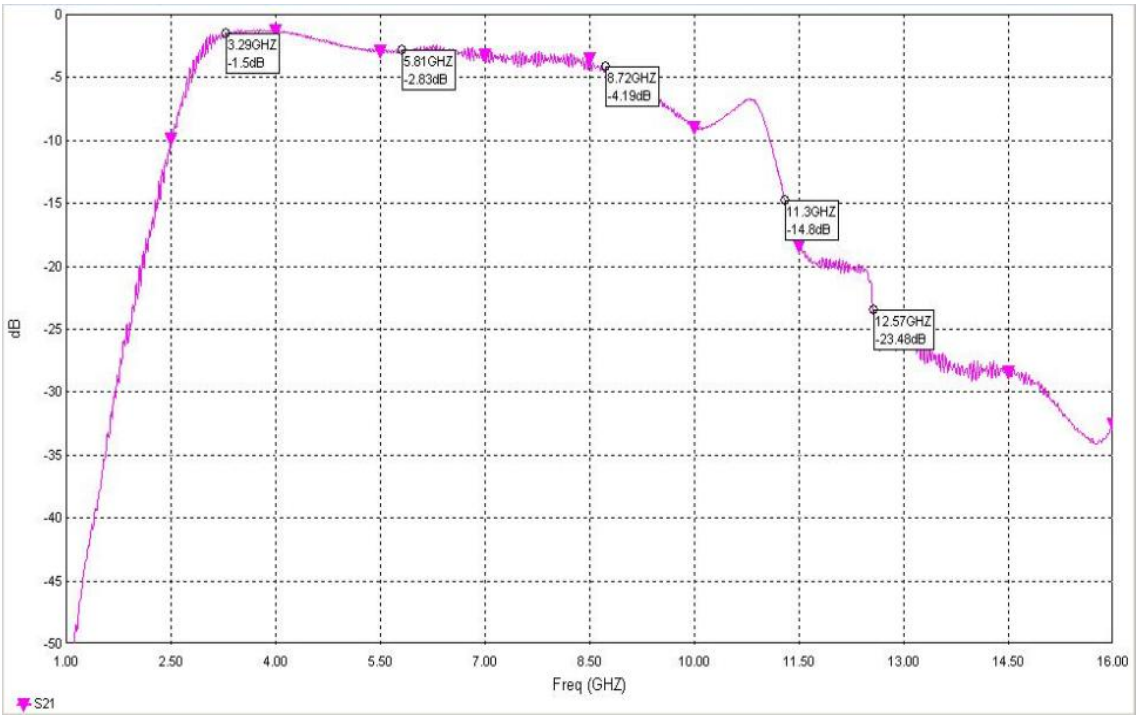

Figure 5.16 Initial test result for S_{21}.

The magnitude of S_{21} is observed to be dropping significantly after 8.5 GHz. The inductance of the via connected the shorted stub to the ground was calculated and is found to be 0.765 nH. This value of inductance when included as parasitic in Sonnet simulation gave comparable results, confirming that the via inductance significantly degrades the transmission characteristics. It is found that a minimum of five parallel vias are required to reduce the effective inductance and to provide reasonable pass band performance. But due to fabrication limitations, the maximum number of vias that could be drilled in the PCB is three. The final test result after having three vias per stub is shown in Figure 5.17.

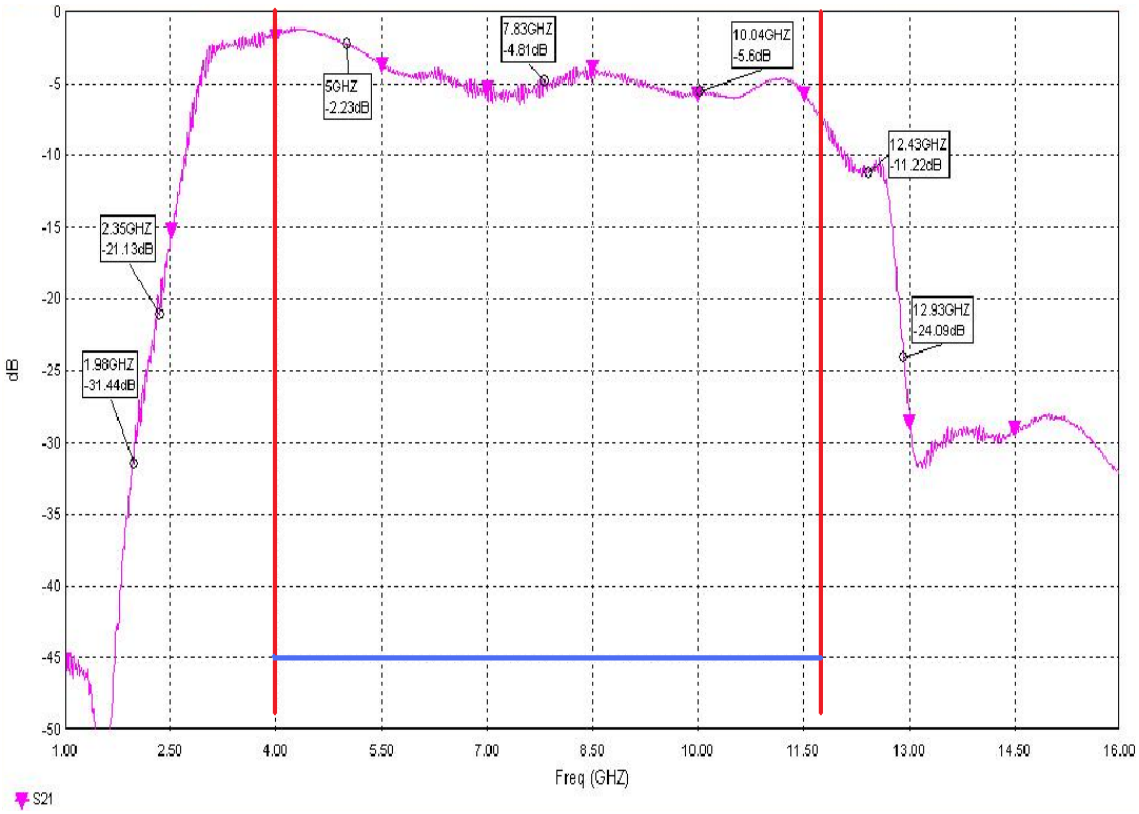

Figure 5.17 Measured S_{21}.

The S_{11} (dB) of the tested filter is shown in Figure 5.18.

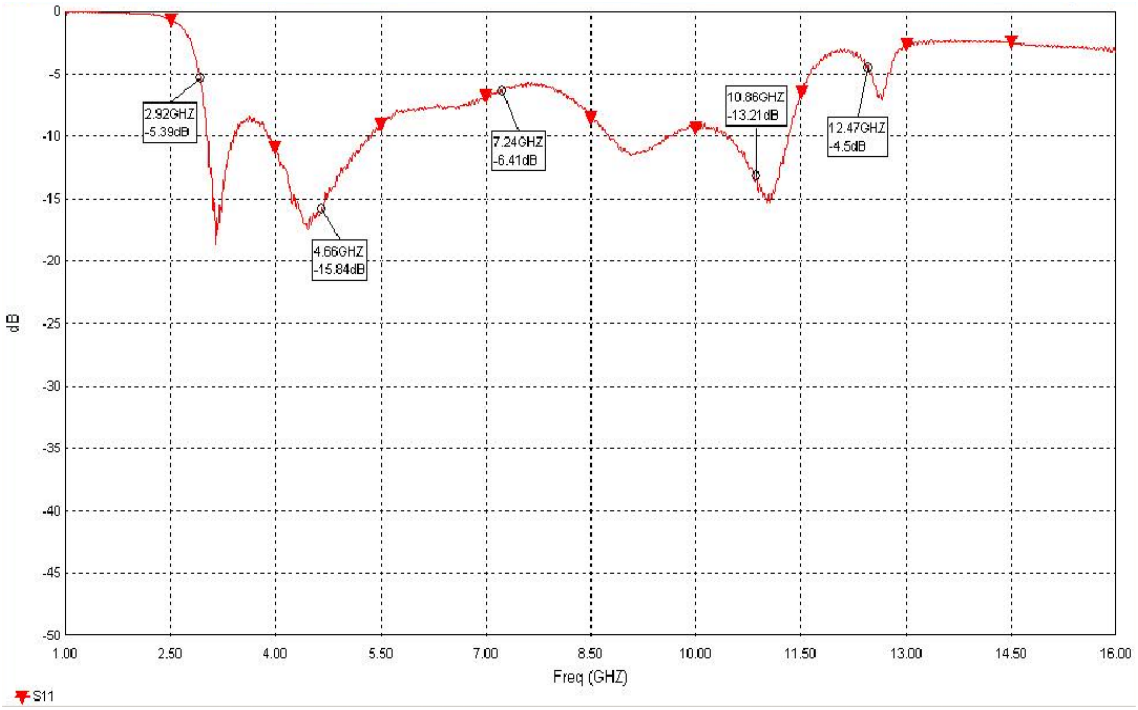

Figure 5.18 Measured S_{11}.

The results confirm that a wide band non-redundant microwave filter can be fabricated with a combination of microstrip single and coupled line techniques. The pass band ripple and losses can be significantly reduced by using accurate fabrication methods. A crude method was used here to fabricate this board to show proof of principle. Along with this, realization of an ideal short-circuited stub is critical for the reliable performance of the filter.

CHAPTER 6

CONCLUSION

An ultra wide band (UWB) non-redundant microwave filter (FBW-Fractional Band Width=100%) is synthesized and the difficulty in realizing series capacitance in planar microstrip technology is discussed. The parallel plate transmission line is a potential solution to this problem since it can give high line characteristic impedance for reasonable physical width. Analysis was is given to prove that the bandwidth of such a structure is severely limited for high impedance lines. An edge coupled structure is used instead to simulate the band-pass characteristic of the series element. Analyses was given to arrive at the coupler impedances are given. The two structures (single and coupled line) are then combined to produce the required band-pass characteristic from 4-12 GHz.

The calculations are verified using ADS as well as Sonnet. Simulations prove that the microstrip and coupled line filters can be combined to give ultra wide band widths. The filter is the optimum filter since no new extra ‘redundant’ elements are added to achieve the response. This method can lead to filters with low insertion loss and wide bandwidth.

The fabricated filter is tested using a network analyzer and the effect of parasitic lead inductance of the shorted stub is discussed. Finally, a filter with three parallel ground shorts is fabricated and the results are included.

The physical filter retains the advantage of planar microstrip technology, compact in size and has excellent frequency response.

REFERENCES

[1] D. Pozar, *Microwave Engineering*. New York: Wiley, 1997.

[2] Terry Edwards, *Foundations for microstrip circuit design*. New York: Wiley- Interscience, 1991.

[3] W. A. Davis, *Microwave semiconductor circuit design*. New York: Van Nostrand, 1984.

[4] W. J. Getsinger, "Microstrip Dispersion Model," IEEE Trans, MTT-21, 1973, pp. 34-39.

[5] Reinhold Ludwig, Gene Bogdanov, *RF Cicuit Design,* NJ: Prentice Hall, 2007.

[6] Thomas Lee, *Planar Microwave Engineering*, Cambridge University Press, 2004.

[7] M.C Horton, R.J Wenzel,*" General theory and design of optimum Quarter-Wave TEM Filters"*, IEEE transactions on Microwave Theory and Techniques.

[8] R. W. Beatty, and D. M. Kerns, *Relationships between different kinds of network parameters, not assuming reciprocity or equality of the waveguide or transmission line characteristic impedances, Proc IEEE (Correspondence*), vol 52, Jan 1964, p 84.

[9] R. K. Mongia, I. J. Bahl, P. Bhartia and J. Hong, *RF and microwave coupled-line circuits*. Norwood, MA: Artech House, 2007.

[10] K. C Gupta, Ramesh Garg, Inder Bahl, Prakash Bhartia , *Microstrip Lines and slot lines*. Norwood , MA: Artech House,1996.

[11] Srinidhi V Kaveri, *Design of tunable edge coupled microstrip band-pass filters, Utah state university, 2008.*

[12] Peter A. Rizzi., *Microwave engineering-passive circuits,* NJ: Prentice Hall, 1988.

[13] G. L. Matthaei, L. Young, and E.M.T Jones, *Microwave Filters, Impedance-Matching Networks, and Coupling Structures*, Artech House, Dedham, Mass., 1980.

[14] E. M. T Jones and J. T. Bolljahn, "*Coupled Strip Transmission Line Filters and Directional Couplers," IRE Trans. Microwave Theory and Techniques*, vol. MTT-4, pp. 78-81, April 1956.

[15] Sang-Gyu Kim, Kai Chang. "*Ultra-wide band transitions and new microwave components using double sided parallel strip lines"*, IEEE transaction on Microwave Theory and Techniques, Vol. 52, NO.9, September 2004.

[16] E. Hammerstad, and O. Jenson, "*Accurate Models for Microstrip Computer-Aided Design*", *IEEE MTT-S Int. Microwave Symp. Dig., 1980,* pp. 407-409.

[17] R. Garg, and I. J. Bahl, "Characteristics of Coupled Microstrip Lines," *IEEE Trans. Microwave Theory and Tech.,* Vol. MTT-27, July 1979, pp. 700-705.

[18] M. Kirschning, and R. H. Jansen, "*Accurate Wide-Range Design Equations for the Frequency-Dependent Characteristics of Parallel Coupled Microstrip Lines*," *IEEE Trans. Microwave Theory Tech.,* Vol. MTT-32, January 1984, pp. 83-90. Corrections: IEEE *Trans. Microwave Theory Tech.,* March 1985, p.288.

[19] E. O. Hammerstad, E. O., and F. Bekkadal, "*A microstrip handbook",* ELAB Reprt, STF 44, A74169, N7034, University of Trondheim-NTH, Norway, 1975.

[20] R. Garg, P. Bhartia, I. Bahl, and A. Ittipiboon, *Microstrip Antenna Design Handbok. Norwood, MA: Artech House, 2001.*

[21] H. A. Wheeler, "*Transmission-Line properties of parallel strips separated by a dielectric sheet,"* IEEE transactions in microwave theory and techniques, MTT-14, No. 2, March 1965, pp. 172-185.

[22] H. A. Wheeler, "*Transmission-Line properties of parallel strips separated by conformal-mapping approximation,"* IEEE transactions in microwave theory and techniques, Vol. MTT-12, May 1964, pp. 280-289.

BIOGRAPHICAL INFORMATION

Vinoj Pillai was born in the state of Kerala, India in March 1980. He received his Bachelor of Technology from NSS Engineering College, Palakkad, Calicut University, Kerala, in 2001. He worked in State Electricity Board, Indian Space Research Organization (ISRO) and Hindustan Aeronautics (HAL) in Bangalore, India and for Transgulf Electromechanical LLC in Dubai UAE. The author commenced his graduate studies in Electrical Engineering department at the University of Texas Arlington in Fall 2007 to achieve expertise in the field of RF/Microwave and Power system design. During his graduate studies, he was a teaching assistant for graduate and undergraduate courses for Dr. Alan Davis and Dr. Kambiz Alavi. His interests include RF/Microwave circuit design, Power system studies, Renewable Energy.